



## UvA-DARE (Digital Academic Repository)

### Life at the extreme

*Plant-driven hotspots of soil nutrient cycling in the hyper-arid core of the Atacama Desert*

Jones, D.L.; Fuentes, B.; Arenas-Díaz, F.; Remonsellez, F.; van Hall, R.; Atkinson, B.S.; Mooney, S.J.; Bol, R.

#### DOI

[10.1016/j.soilbio.2023.109128](https://doi.org/10.1016/j.soilbio.2023.109128)

#### Publication date

2023

#### Document Version

Final published version

#### Published in

Soil Biology and Biochemistry

#### License

CC BY

[Link to publication](#)

### Citation for published version (APA):

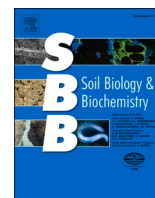
Jones, D. L., Fuentes, B., Arenas-Díaz, F., Remonsellez, F., van Hall, R., Atkinson, B. S., Mooney, S. J., & Bol, R. (2023). Life at the extreme: Plant-driven hotspots of soil nutrient cycling in the hyper-arid core of the Atacama Desert. *Soil Biology and Biochemistry*, 184, Article 109128. <https://doi.org/10.1016/j.soilbio.2023.109128>

### General rights

It is not permitted to download or to forward/distribute the text or part of it without the consent of the author(s) and/or copyright holder(s), other than for strictly personal, individual use, unless the work is under an open content license (like Creative Commons).

### Disclaimer/Complaints regulations

If you believe that digital publication of certain material infringes any of your rights or (privacy) interests, please let the Library know, stating your reasons. In case of a legitimate complaint, the Library will make the material inaccessible and/or remove it from the website. Please Ask the Library: <https://uba.uva.nl/en/contact>, or a letter to: Library of the University of Amsterdam, Secretariat, Singel 425, 1012 WP Amsterdam, The Netherlands. You will be contacted as soon as possible.



## Life at the extreme: Plant-driven hotspots of soil nutrient cycling in the hyper-arid core of the Atacama Desert

Davey L. Jones<sup>a,b,\*</sup>, Bárbara Fuentes<sup>c</sup>, Franko Arenas-Díaz<sup>d</sup>, Francisco Remonsellez<sup>e</sup>, Rutger van Hall<sup>f</sup>, Brian S. Atkinson<sup>g</sup>, Sacha J. Mooney<sup>g</sup>, Roland Bol<sup>h,a</sup>

<sup>a</sup> SoilsWales, School of Natural Sciences, Bangor University, Gwynedd, LL57 2UW, UK

<sup>b</sup> SoilsWest, Centre for Sustainable Farming Systems, Food Futures Institute, Murdoch University, Murdoch, WA 6150, Australia

<sup>c</sup> Departamento de Ingeniería Química, Universidad Católica del Norte, Antofagasta, Chile

<sup>d</sup> Programa de Doctorado en Ciencias mención Geología, Departamento de Cs. Geológicas, Universidad Católica del Norte, Antofagasta, Chile

<sup>e</sup> Centro de Investigación Tecnológica del Agua en el Desierto-CEITSAZA, Universidad Católica del Norte, Antofagasta, Chile

<sup>f</sup> Institute for Biodiversity and Ecosystem Dynamics, University of Amsterdam, Science Park 904, 1090 GE, Amsterdam, the Netherlands

<sup>g</sup> Agricultural and Environmental Sciences, School of Biosciences, University of Nottingham, Nottingham, LE12 5RD, UK

<sup>h</sup> Institute of Bio- and Geosciences, Agrosphere Institute (IBG-3), Forschungszentrum Jülich, 52425, Jülich, Germany

### ARTICLE INFO

#### Keywords:

Astrobiology  
Biological hotspot  
Nutrient cycling  
Desert microbiology  
Moisture availability  
Yungay region

### ABSTRACT

The hyperarid core of the Atacama Desert represents one of the most intense environments on Earth, often being used as an analog for Mars regolith. The area is characterized by extremes in climate (e.g., temperature, humidity, UV irradiation) and edaphic factors (e.g., hyper-salinity, high pH, compaction, high perchlorates, and low moisture, phosphorus and organic matter). However, the halophytic C<sub>4</sub> plant *Distichlis spicata* appears to be one of the few species on the planet that can thrive in this environment. Within this habitat it captures windblown sand leading to the formation of unique structures and the generation of above-ground phyllosphere soil. Using a combination of approaches (e.g., X-ray Computed Tomography, TXRF,  $\delta^{13}\text{C}/\delta^{15}\text{N}$  isotope profiling, microbial PLFAs,  $^{14}\text{C}$  turnover, phosphate sorption isotherms) we examined the factors regulating the biogeochemical cycling of nitrogen (N), phosphorus (P) and carbon (C) in both vegetated and unvegetated areas. Our results showed that *D. spicata* rhizomes with large aerenchyma were able to break through the highly cemented topsoil layer leading to root proliferation in the underlying soil. The presence of roots increased soil water content, P availability and induced a change in microbial community structure and promoted microbial growth and activity. In contrast, soil in the phyllosphere exhibited almost no biological activity. Organic C stocks and recent C<sub>4</sub> plant derived input increased as follows: phyllosphere (1941 g C m<sup>-2</sup>; 85% recent) > soils under plants (575–748 g C m<sup>-2</sup>; 55–60%) > bare soils (491–642 g C m<sup>-2</sup>; 9–17%). Due to the high levels of nitrate in soil (>2 t ha<sup>-1</sup>) and high rates of P sorption/precipitation, our data suggest that the microbial activity is both C and P, but not N limited. Root-mediated salt uptake combined with foliar excretion and dispersal of NaCl into the surrounding area indicated that *D. spicata* was responsible for actively removing ca. 55% of the salt from the rhizosphere. We also demonstrate that NH<sub>3</sub> emissions may represent a major N loss pathway from these soil ecosystems during the processing of organic N. We attribute this to NH<sub>3</sub> volatilization to the high pH of the soil and slow rates of nitrification. In conclusion, we demonstrate that the extremophile *D. spicata* physically, chemically and biologically reengineers the soil to create a highly bioactive hotspot within the climate-extreme of the Atacama Desert.

### 1. Introduction

Hyper-arid environments are defined by an extremely low rainfall (annual precipitation of less than 60–100 mm), high evapotranspiration

and an overall aridity index of <0.05 (UNEP 1997). Hyper-aridity not only severely limits the development of vegetation but also leads to soils that are significantly affected by salts (e.g. NaCl, KNO<sub>3</sub>, NaClO<sub>4</sub>; Wang et al., 2017). As salt accumulates in the superficial horizons due to high

\* Corresponding author. SoilsWales, School of Natural Sciences, Bangor University, Bangor, Gwynedd, LL57 2UW, UK.

E-mail address: [d.jones@bangor.ac.uk](mailto:d.jones@bangor.ac.uk) (D.L. Jones).

<https://doi.org/10.1016/j.soilbio.2023.109128>

Received 6 June 2023; Received in revised form 10 July 2023; Accepted 19 July 2023

Available online 25 July 2023

0038-0717/© 2023 The Authors. Published by Elsevier Ltd. This is an open access article under the CC BY license (<http://creativecommons.org/licenses/by/4.0/>).

evapotranspiration and lack of precipitation, no leaching to deeper layers of the soil occurs leading to highly stratified soil profiles (Fuentes et al., 2022a). Despite the inhospitable conditions prevailing in hyper-arid environments, life exists, indicative that the biogeochemical recycling of key nutrients (C, N and P) can take place (Knief et al., 2020; Fuentes et al., 2022b). However, biogeochemical cycling is extremely heterogeneous, being concentrated in discrete spatial and temporal hotspots of activity. For example, Ewing et al. (2008) showed that in arid and hyper-arid soils, rapid cycling of C occurs in spatially segregated patches at the soil surface with plants exerting strong control on the supply of organic C. In addition, several studies have reported plants and associated microbial communities in hyper-arid environments both participate in soil nutrient cycling and in the rapid turnover of carbon (C) and nitrogen (N), particularly in response to ephemeral inputs of moisture (Jones et al., 2018a,b; Santander et al., 2021; Wu et al., 2021).

The hyper-arid zone of the Atacama Desert is widely studied due to its unique aridity and the presence of microbial and plant extremophiles (Uritskiy et al., 2019; Morales-Tapia et al., 2021). Among its other attributes, its soil properties are often used as a proxy for the exploration of Mars and the search for life on other planets (Ewing et al., 2006; Azúa-Bustos et al., 2012; Fletcher et al., 2012). Within the hyper-arid core of the Atacama Desert, the southern margin, known as Yungay, is frequently studied due to its extreme climate (Warren-Rhodes et al., 2006) with this region generally devoid of vegetation and considered absolute desert (Cáceres et al., 2007). Within Yungay, however, very small patches of halophytic vegetation do exist on a desert alluvial fan within the Quebrada del Profeta which have become colonized by shrubs, predominantly *Distichlis spicata* (L.) Greene (Ingendesa, 1997). The plant and edaphic factors that enable *D. spicata* to survive in one of the most extreme environments on Earth, however, are lacking. Unlike many ecosystems, plants in the Atacama Desert are rarely N limited due to the presence of extensive potassium and sodium nitrate deposits at the soil surface (Sutter et al., 2007; Voigt et al., 2020).

Plants that survive in the Atacama desert contribute to the emergence of highly heterogeneous landscapes, along with generating fertility islands and biodiversity hotspots (Castillo et al., 2017). Such areas are typically characterized by soils with higher moisture and nutrient content, as well as, enhanced microbial activities compared with the surrounding bare soils (Garner and Steinberger, 1989; Kidron, 2009; Gao et al., 2022). The plants themselves provide niches for microbial communities to thrive including bacteria, fungi, protists, nematodes and viruses (Trivedi et al., 2020). These above-ground niches include the phyllosphere and leaf endosphere, while below ground they include the endo- and ecto-rhizosphere (Araya et al., 2020; Arndt et al., 2020). In the case of *D. spicata*, its above-ground stems and foliage also captures a large amount of wind-blown soil, leading to the formation of a unique plant structure and the formation of large amounts of phyllosphere soil suspended above the traditional soil surface. Although not yet demonstrated in the Atacama desert, other niches promoted by the presence of plants may include endolithic microbial communities and biocrusts due to the provision of shade, enhanced humidity and the buffering of climate extremes (She et al., 2022).

In hyper-arid regions, the above-ground habitat for microorganisms are directly influenced by plant metabolism, however, abiotic factors are thought to dominate colonization potential (e.g., temperature, relative humidity, solar radiation, dust input) (Compant et al., 2019; Liu et al., 2023). In comparison, microbial communities below-ground in hyper-arid soils are likely to be more shaped by biotic factors (i.e., plant litter inputs, root exudation, symbiotic associations) as well as abiotic factors (i.e., soil type, moisture, temperature pH, salinity, nutrient availability) (Alfaro et al., 2021).

Given the paucity of information on extremophile plant-soil interactions in hyper-arid ecosystems, the objective of this study was to (i) evaluate microbial activity and biogeochemical cycling in the presence and absence of *D. spicata* plants, (ii) compare the properties of topsoil and subsoils in comparison to soil accumulated above-ground in the

phyllosphere.

## 2. Materials and methods

### 2.1. Site description

The study site was located within the Yungay area, in the hyper-arid core of the Atacama Desert at Oficina Yugoslavia, Antofagasta, Chile (24°3'28"S, 69°49'33"W; 948 m above sea level) (Figs. S1–S2). It receives <2 mm rain per year and has a mean annual temperature of 14–16 °C with a maximum of 37.9 °C and minimum of –5.7 °C (Warren-Rhodes et al., 2006; McKay et al., 2003). The extremely infrequent rainfall events can leave free water in the surface soil for ca. 3 d while it takes 10 d for the soil water content to revert back to pre-rainfall conditions (McKay et al., 2003). The relative humidity of the air at the site can vary from 1 to 95% depending on the presence of atmospheric fogs (Cáceres et al., 2007; Azúa-Bustos et al., 2011). The site experiences some of the most extreme potential evapotranspiration rates (ca. 1–2 mm d<sup>-1</sup>; Mintz and Walker 1993), surface UV radiation and total solar irradiances measured on Earth (Cordero et al., 2018; Rondanelli et al., 2015). Geomorphic studies suggest that the field site has experienced a near-continuous hyperarid climate since the late Pliocene (3 Mya; Amundson et al., 2012).

The zone of study is in a low-lying position and experiences sporadic drainage from torrential but very infrequent rainfall events which has led to the creation of an alluvial fan composed of gravels and lenses of unconsolidated coarse sand (Ferrando and Espinoza, 2013; Pfeiffer et al., 2021). The site is located over a desert alluvial fan cut by the Quebrada del Profeta in which a series of dry stream beds have become colonized by higher plants, predominantly *D. spicata* (L.) Greene (Poaceae; common name: Grama salada or Desert saltgrass)(Figs. S3–S4). Away from the streambed, no plant colonization occurred suggesting that this was an ephemeral moisture hotspot within the landscape (Fig. S3). Although the site is located within the hyper-arid core of the Atacama Desert, we established that groundwater is located 6 m below the ground surface (at location 24°03'12"S, 69°49'18"W). Plants were present in two distinct growth forms: (i) plants low to the ground (mean shoot height 12 ± 3 cm,  $n = 20$ ), or (ii) plants in dense upright columns (mean height 112 ± 6 cm, mean width 78 ± 8 cm;  $n = 5$ ; Fig. S3). These columns consist of dense clumps of stems that facilitate the accretion of windblown dust (i.e., phyllosphere soil), however, some soil may also have been eroded from the base of the plants during past torrential rain events (Fig. S4). This study only focused on the column forms of *D. spicata*.

### 2.2. Sample collection

Individual similar-sized columns of *Distichlis spicata* ( $n = 5$ ) were randomly selected within a 100 × 100 m study area. The columns were located in different braids of the dry stream bed system. In addition, adjacent areas at least 5 m distant from the columns but containing no plants were used as reference controls ( $n = 5$ ; Fig. S5). At each sampling location, 10 green shoots (12.3 ± 0.8 cm long), 10 senescent brown shoots (11.1 ± 1.0 cm long), short sections of stem (ca. 5 cm in length; diameter 3.18 ± 0.14 mm,  $n = 10$ ) and roots were recovered from each plant column. Root samples composed a composite of rhizomes (diameter 2.45 ± 0.26 mm,  $n = 10$ ), primary roots (diameter 0.54 ± 0.03 mm,  $n = 10$ ) and secondary roots (diameter 0.28 ± 0.01 mm,  $n = 10$ ) relative to their abundance in the field. In addition, samples of the Atacama endemic shrubs *Atriplex atacamensis* Phil. (Amaranthaceae) ( $n = 4$ ), *Adesmia atacamensis* Phil. (Fabaceae) ( $n = 2$ ) and the tree *Prosopis tamarugo* Phil. (Fabaceae) ( $n = 1$ ) growing at the study site were collected as reference controls for isotopic end-member analysis and nutrient comparisons.

The soil at the site is classified as a hyperaridic Typic Haplosolud (Finstad et al., 2014). Soil samples were collected at depth of 5–20 cm

and 20–40 cm below the soil surface (with and without and *D. spicata* present). Unlike the top 0–5 cm, soil in these layers was not cemented and showed an abundance of roots in the *D. spicata* samples. No roots were observed in the bare soil controls. Additionally, soil samples of phyllosphere soil were taken from inside each of the *D. spicata* plant columns at a height of ca. 70 cm above the soil surface (Figs. S4–S6; Table S1). Intact soil samples containing roots were also collected from the cemented layer (ca. 0–5 cm) at base of the *D. spicata* plants. This sampling regime is shown schematically in Figs. S6–S7.

### 2.3. Soil and canopy temperature and humidity

To monitor diurnal patterns in soil temperature and relative humidity (RH), DS1923-F5 Hygrochron temperature and humidity data loggers (iButtonLink LLC, Whitewater, WI) were placed in the soil at two depths (1 cm, 10 cm) and within the vegetation canopy (phyllosphere soil). Data was recorded hourly from October 2018 to March 2019 (6 months). The accuracy of the thermal measurements is  $\pm 0.5$  °C and the RH measurements  $\pm 3.5\%$ .

### 2.4. Plant analysis

Root and stem diameters were determined by image analysis. Plant moisture content was determined by oven-drying (80 °C, 48 h) and then ground to a fine powder using a MM200 ball mill (Retsch GmbH, Haan, Germany). Subsequently, their elemental composition was determined using a non-destructive S2 Picofox TXRF spectrometer (Bruker Inc., Billerica, MA) using Ga as an internal standard and validated using a range of certified plant standards (WEPAL-QUASIMEME, Wageningen, The Netherlands). The C, N,  $\delta^{13}\text{C}$  and  $\delta^{15}\text{N}$  contents of the milled plant samples were determined using a Vario Isotope cube connected with a BioVision Element continuous flow Isotope Ratio Mass Spectrometer (Elementar GmbH, Langselbold, Germany). Total C and N content were determined by peak integration as well as calibration against elemental standards. At least two calibrated laboratory standards were used to ensure the quality of analyses and to scale normalize the raw values to the international isotopic reference VPDB ( $^{13}\text{C}$ ) and AIR ( $^{15}\text{N}$ ). The standards were run before, in between and after the samples. Within the instrument software they were evaluated and used to calibrate the instrument on each run, do linearity checks and correction (as per de Groot, 2004) and required drift corrections. Standards included: lithium carbonate ( $^{13}\text{C}$ ), IAEA-NBS18, calcite ( $^{13}\text{C}$ ), IAEA-600, caffeine ( $^{13}\text{C}$ ), IAEA-CH6, sucrose ( $^{13}\text{C}$ ), IAEA-N2, ammonium sulfate ( $^{15}\text{N}$ ) or IAEA-USGS-25, ammonium sulfate ( $^{15}\text{N}$ ). The general precision of replicate analyses is estimated to be better than 5% (rel.) for C and N content and  $<0.1\%$  for  $\delta^{13}\text{C}$  and  $\delta^{15}\text{N}$  content.

### 2.5. Soil characterisation

Samples were shipped to the UK under the UK Department for Environment, Food & Rural Affairs plant health import licence number 52025/198560-6 in plastic containers. Upon arrival, moisture content was determined gravimetrically by oven drying (105 °C, 48 h). The chemical characteristics of the soils was determined by firstly shaking (200 rev  $\text{min}^{-1}$ , 30 min) 10 g of field-moist soil with 25 ml of distilled water. The pH and electrical conductivity (EC) of the extracts was then determined using standard electrodes. The extracts were then centrifuged (24,000 g, 5 min) and the supernatant recovered. These were subsequently used for the analysis of soluble salts (Na, K, Ca) using a Sherwood 410 flame photometer (SciMed Ltd, Stockport, UK), P using the molybdate blue colorimetric procedure of Murphy and Riley (1962),  $\text{NO}_3^-$  using the vanadate colorimetric procedure of Miranda et al. (2001),  $\text{NH}_4^+$  using the salicylate-based colorimetric method of Mulvaney (1996), total phenolics using the Folin-Ciocalteu procedure of Swain and Hillis (1959), and dissolved organic C (DOC) and N (DON) using an Multi N/C 2100S analyzer (Analytik Jena GmbH, Jena, Germany).

$\text{CaCO}_3$  content was determined with a FOGL Benchtop Soil Calcimeter (BD Inventions, Thessaloniki, Greece). P sorption isotherms were determined by shaking different concentrations of  $\text{K}_2\text{H}^{33}\text{PO}_4$  (5 ml, 5–280  $\text{mg P l}^{-1}$ , 2.6 kBq) with 1 g of field-moist soil at 200 rev  $\text{min}^{-1}$  for 24 h. The suspensions were then centrifuged (18,000 g, 5 min) and the equilibrium P concentration determined by liquid scintillation counting using Optiphase HiSafe 3 scintillation fluid and a Wallac 1404 scintillation counter with automated quench correction (PerkinElmer Inc., Waltham, MA). The P buffer power ( $B_p$ ) was calculated according to Barber (1995; see Supp Info). Available P was determined using 2 methods: (i) Olsen P method (0.5 M  $\text{NaHCO}_3$  pH 8.5, 1:5 w/v extract; FAO, 2021), and (ii) acetic acid method (0.5 M  $\text{CH}_3\text{COOH}$  pH 2.5, 1:5 w/v extract (McCray et al., 2012). The sand, clay and silt particle size distribution was determined through textural analysis using a Micromeritics particle size analyser.

Comparable to plant samples analysis, soils were ground to a fine powder using a MM200 ball mill and then decalcified using 4 M HCl by adding enough acid until the samples finished bubbling. To get rid of the excess acid and moisture, the samples were freeze dried after which each sample was homogenized before weighing in for the subsequent EA-IRMS analysis as described above for the plant samples.

The percentage of new (here  $\text{C}_4$ -derived) carbon in the soil ( $F$ ) was calculated as:

$$F = ((\delta^{13}\text{C}_{\text{soil}} - \delta^{13}\text{C}_{\text{C3soil}}) / (\delta^{13}\text{C}_{\text{C4soil}} - \delta^{13}\text{C}_{\text{C3soil}})) \times 100$$

with  $\delta^{13}\text{C}_{\text{soil}}$  =  $\delta^{13}\text{C}$  value of the actual soil or phyllosphere sample,  $\delta^{13}\text{C}_{\text{C3soil}}$  = the  $\delta^{13}\text{C}$  value of  $\text{C}_3$  soil endmember (set at  $-26\%$ ) and  $\delta^{13}\text{C}_{\text{C4soil}}$  =  $\delta^{13}\text{C}$  value of  $\text{C}_4$  soil endmember (set at  $-12\%$ ). For more details see Balesdent et al. (1987). Plants with  $\text{C}_3$  photosynthesis have  $\delta^{13}\text{C}$  values ranging from approximately  $-32$  to  $-22\%$  (mean ca.  $-27\%$ ), while those with  $\text{C}_4$  photosynthesis have values ranging from about  $-17$  to  $-9\%$  (mean ca.  $-13\%$ ) (Boutton et al., 1998). Studies by Diefendorf et al. (2010) and Kohn (2010) highlight that desert  $\text{C}_3$  plants are expected to have  $\delta^{13}\text{C}$  values above the global mean.

### 2.6. X-ray Computed Tomography (CT)

Samples were extracted from the soil as intact blocks of soil using a spade and placed in plastic boxes with packaging material to preserve the soil structure. These were then transported to the UK. Representative specimens of intact soil from the hard cemented soil surface layer (0–5 cm) were scanned on a Phoenix VtomeX M 240 high resolution X-ray CT system (Waygate Technologies, Wunstorf, Germany) at the Hounsfield Facility, University of Nottingham, UK. The scanning parameters were optimized to allow balance between a large field of view and a high resolution. Each sample was imaged using a voltage and current of 170 kV and 160  $\mu\text{A}$  respectively at a voxel size resolution of 58  $\mu\text{m}$ . The specimen stage was rotated through  $360^\circ$  at a step increment of  $0.143^\circ$  over 36 min thus a total of 2520 projection images were obtained by averaging 3 frames (with 1 skip) with an exposure of 200 ms each, at every rotation step. Each scan was then reconstructed using DatosRec software (Waygate Technologies, Wunstorf, Germany). Radiographs were visually assessed for sample movement before being reconstructed in 16-bit depth volumes with a beam hardening correction of 6. Reconstructed volumes were then submitted for visualization in VG Studio MAX (version 2.2.0; Volume Graphics GmbH, Heidelberg, Germany).

Images of the soil specimens was undertaken using Image J (FiJI 64-bit). An assessment of each sample was undertaken by first creating a region of interest (ROI) for comparison between samples. Within each region, the separate segmentation of plant material was undertaken to ensure accurate characterization of soil morphological properties which was performed by creating a 'mask' in VG Studio MAX of the plant material i.e., roots/stems contained within the region of interest. This segmentation process was undertaken via manual application of a region



growing algorithm. Once the ROI was created the Otsu algorithm in Image J was used to binarize the sample (i.e., discriminate the solid and pore space). The sample was then assessed as the entire sample/volume referred to as the bulk soil based on the largest rectangular region that fit within the irregular shaped sample. The samples were then separated visually into low density soil (i.e., high porosity) and high-density soil (i.e. low porosity) regions (considerably smaller than the bulk soil region, for further analysis). The separate regions were then assessed for the following morphological properties; porosity, pore size, pore size distribution and coefficient of uniformity (a ratio of the pore size distribution expressed by  $d_{60}:d_{10}$ ).

## 2.7. Microbial activity and C use efficiency

To evaluate soil microbial activity, field-moist soil (5 g) from each site (topsoil, subsoil, phyllosphere soil) was placed in individual sterile 50 cm<sup>3</sup> polypropylene tubes. <sup>14</sup>C-glucose was then added to each sample (100 µl, 3.86 kBq) at either a low (10 µM; 14 ng C g<sup>-1</sup>) or high rate (10 mM; 14 µg C g<sup>-1</sup>) of C relative to the size of the microbial biomass. To capture the <sup>14</sup>CO<sub>2</sub> released, a NaOH trap (1 ml) was suspended above the soil and the tubes hermetically sealed and incubated at 20 °C. The NaOH trap was replaced periodically over 48 d. The NaH<sup>14</sup>CO<sub>3</sub> in the NaOH traps was determined by liquid scintillation counting as described above. At the end of the incubation period the soils were extracted with 1 M NaCl (1:5 w/v; 200 rev min<sup>-1</sup>, 15 min), centrifuged (18,000 g, 10 min) and the amount of <sup>14</sup>C present in the supernatant determined by liquid scintillation counting. NaCl was used in place of KCl to minimise the background associated with <sup>4</sup>K. Microbial C use efficiency (CUE) for the added substrates was calculated according to Jones et al. (2018a,b), where

$$CUE = \frac{({}^{14}\text{C}_{\text{tot}} - {}^{14}\text{CO}_2 - {}^{14}\text{C}_{\text{NaCl}})}{({}^{14}\text{C}_{\text{tot}} - {}^{14}\text{C}_{\text{NaCl}})} \quad (\text{Eqn. 1})$$

and where <sup>14</sup>C<sub>tot</sub> is the total amount of <sup>14</sup>C-glucose added to the soil, <sup>14</sup>CO<sub>2</sub> is the amount of <sup>14</sup>C-glucose respired and <sup>14</sup>C<sub>NaCl</sub> is the amount of <sup>14</sup>C recovered in the NaCl extract at the end of the experiment (i.e. unused substrate).

We also measured the microbial turnover of complex, plant-derived C across the different soil depths according to Glanville et al. (2012). Briefly, high molecular weight (MW) plant material was prepared by heating 2.5 g of <sup>14</sup>C-labelled *Lolium perenne* L. shoots (Hill et al., 2007) in distilled water (25 ml, 80 °C) for 2 h. The extract was then centrifuged (1118 g, 5 min) and the soluble fraction removed. The pellet was then re-suspended in distilled water and the heating and washing procedure repeated twice more until >95% of the water-soluble fraction had been removed. The pellet remaining was dried overnight at 80 °C and ground to a fine powder. The heating ensured that the intrinsic microbial community in the plant material was minimized Jones et al. (2018a,b). The mineralization dynamics of the high MW plant material was determined by mixing 50 mg of <sup>14</sup>C-labelled plant material (42 kBq g<sup>-1</sup>) with 5 g of field-moist soil. The production of <sup>14</sup>CO<sub>2</sub> was monitored over 48 d as described above for <sup>14</sup>C-labelled glucose.

## 2.8. Soil microbial nitrogen dynamics

Potential net N mineralization was determined by anaerobic incubation according to Waring and Bremner (1964) and Kresović et al. (2005). Briefly, 2 g of field-moist soil was placed in 20 cm<sup>3</sup> polypropylene tubes and anaerobic conditions imposed by filling the tubes with distilled water and then sealing the tubes. Soil samples were then incubated for 10 d in the dark at 40 °C. Subsequently, the incubated samples were transferred to 50 cm<sup>3</sup> polypropylene tubes and solid KCl was added to achieve a final concentration of 1 M KCl. The samples were then extracted by shaking for 30 min (200 rev min<sup>-1</sup>), centrifuged (18000 g, 10 min) and NH<sub>4</sub><sup>+</sup> in the supernatant determined colorimetrically as described previously. Net ammonification was calculated as

the amount of NH<sub>4</sub><sup>+</sup> present after 7 d minus that present at the start of the incubation.

To determine the rate of arginine mineralization, 0.2 ml of a <sup>14</sup>C-labelled L-arginine solution (50 mM; C:N ratio 6:4; 2.17 kBq ml<sup>-1</sup>; 10 µmol g<sup>-1</sup>; 0.56 mg N g<sup>-1</sup>; Amersham Biosciences UK Ltd, Chalfont St Giles, Bucks, UK) was added to 1 g of field-moist soil in a sterile 50 cm<sup>3</sup> polypropylene tube (Kemmitt et al., 2006). A 1 M NaOH trap was suspended above the soil to catch any <sup>14</sup>CO<sub>2</sub> evolved and the traps periodically changed over a 96 h as described above. In addition, a 2.1 cm diameter Whatman GF/C glass fibre filter paper (GE Healthcare Bio-Sciences, Pittsburgh, PA) impregnated with 0.15 M H<sub>3</sub>PO<sub>4</sub> was suspended above the soil to capture any NH<sub>3</sub> emitted from the soil (Jones et al., 2012). At the end of the incubation period the NaOH and H<sub>3</sub>PO<sub>4</sub> traps were removed. Subsequently, the NH<sub>4</sub><sup>+</sup> produced derived from the mineralization of arginine was determined by extracting the soil with 1 M KCl (1:5 w/v) as described previously. The H<sub>3</sub>PO<sub>4</sub> impregnated filter papers in the NH<sub>3</sub> traps were vortexed with 0.9 ml of distilled water, centrifuged (18,000 g, 10 min) and their NH<sub>4</sub><sup>+</sup> content determined colorimetrically as above.

## 2.9. Microbial community structure

Microbial community structure was measured by phospholipid fatty acid (PLFA) analysis following the method of Buyer and Sasser (2012). Briefly, samples (2 g) were freeze-dried and Bligh-Dyer extractant (4.0 ml) containing an internal standard added. Tubes were sonicated in an ultrasonic bath for 10 min at room temperature before rotating end-over-end for 2 h. After centrifuging (10 min) the liquid phase was transferred to clean 13 mm × 100 mm screw-cap test tubes and 1.0 ml each of chloroform and water added. The upper phase was removed by aspiration and discarded while the lower phase, containing the extracted lipids, was evaporated at 30 °C. Lipid classes were separated by solid phase extraction (SPE) using a 96-well SPE plate containing 50 mg of silica per well (Phenomenex, Torrance, CA). Phospholipids were eluted with 0.5 ml of 5:5:1 methanol:chloroform:H<sub>2</sub>O (Findlay, 2004) into glass vials, the solution evaporated (70 °C, 30 min). Transesterification reagent (0.2 ml) was added to each vial, the vials sealed and incubated (37 °C, 15 min). Acetic acid (0.075 M) and chloroform (0.4 ml each) were added. The chloroform was evaporated just to dryness and the samples dissolved in hexane. The samples were analyzed with a 6890 gas chromatograph (Agilent Technologies, Wilmington, DE) equipped with autosampler, split-splitless inlet, and flame ionization detector. Fatty acid methyl esters were separated on an Agilent Ultra 2 column, 25 m long × 0.2 mm internal diameter × 0.33 µm film thickness. Standard nomenclature was followed for fatty acids (Frostegård et al., 1993) with affiliation of individual fatty acids to taxonomic groups undertaken as described in Table S3.

## 2.10. Statistical analysis

Differences in major plant and soil characteristics were determined by a One-way or two-way ANOVA, as appropriate, using Minitab v18.0 (Minitab Inc., State College, PA).  $P < 0.05$  was used as the cut-off for statistical significance. Differences in soil microbial community structure were evaluated with principal component analysis in Minitab v18.0. Linear regression was used to evaluate relationships between variables in Minitab v18.0. Values in the text represent means ± SEM unless otherwise stated.

## 3. Results

### 3.1. Temperature and relative humidity of the plant canopy and the soil

As expected, distinct diurnal patterns were apparent in the climate data (Fig. 1). Overall, daytime mean temperatures values were similar over the 6-month period being 21.6 °C in the plant canopy, 25.1 °C in the

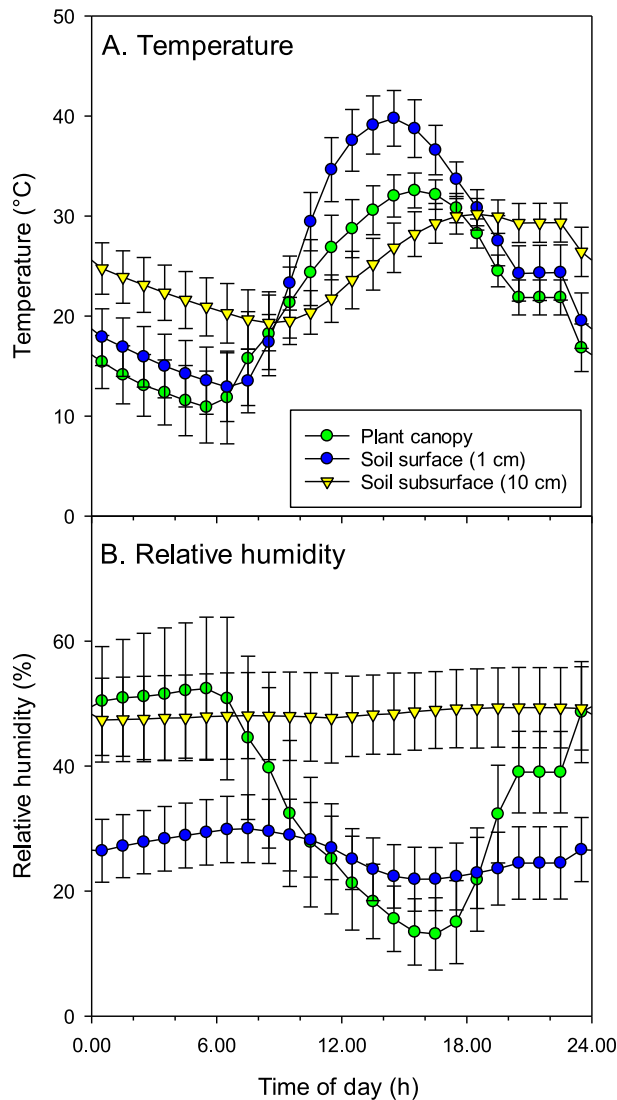


**Fig. 1.** Temperature and relative humidity of the air in the above-ground plant canopy, soil surface (0–1 cm) and subsurface (10 cm) layers at the field site in the Atacama Desert.

surface soil and 24.8 °C in the subsurface soil. The mean daily oscillation in temperature, however, was largest in the surface soil (26.8 °C), followed by the plant canopy (21.7 °C), with much less temperature variation seen in the subsurface soil (10.9 °C). The highest average temperatures in the plant canopy, surface soil and subsurface soil were recorded between 13:00 and 15:00 h and reached 36.6 °C, 45.0 °C and 36.1 °C, respectively (Fig. 1A). The minimum temperatures were seen between 05:00–06:00 h reaching a low of 3.6 °C, 6.5 °C, and 11.1 °C in the plant canopy, surface soil and subsurface soil, respectively (Table S2, Fig. S9).

The relative humidity (RH) was relatively constant in the soil and was always higher in the subsurface soil, with average values in the range of 47 and 49%; while lower values in the range of 21–29% were found in the surface soil (Fig. 1). The RH in the plant canopy reached its highest values at night until 06:00 h with values around 50%, then decreased sharply during daylight hours. The mean daily oscillation in RH was largest in the plant canopy (39.2%), while the daily variation in the surface and subsurface soil was much lower being 8.1% and 2.0%, respectively. The minimum and maximum RH recorded in the plant

canopy was 3.6% and 77.7%, respectively (Table S2, Fig. S9).

### 3.2. Plant analyses

The macro- and micronutrient content of the different plant parts of *D. spicata* were significantly different for all analyzed elements, except S (fresh leaves, senescent leaves, stems and roots; Table 1). Analysis also confirmed that the fresh leaves contained high levels of NaCl with an abundance of salt crystals on the leaf surface (Fig. S10), with the highest levels seen in the photosynthetic leaves. The C/N ratio of the *D. spicata* leaves was higher than of the leaves of the other 3 species. The  $\delta^{15}\text{N}$  content of *D. spicata* plant parts (12.0–21.7‰) was higher than leaves of the other 3 species (5.8–11.9‰) (Table 1; Figs. S10–11). Above and below ground plant  $^{13}\text{C}$  values reflected their  $\text{C}_3$ , *Adesmia atacamensis* (-25.2‰) and *Prosopis tamarugo* (-23.5‰) or  $\text{C}_4$  photosynthetic pathway, *D. spicata* and (-13.2 to -15.3‰) and *Atriplex atacamensis* (-15.0‰) (Table 1; Fig. S10).

### 3.3. Soil analysis

#### 3.3.1. Soil elemental and nutrient content

There was no significant difference in soil textural properties (i.e. clay, silt or sand content), in areas with and without *D. spicata* plants (Table 2). However, there were significant differences for most of the other measured parameters, excepting  $\text{NO}_3^-$ , between the two sampled areas (with plants and without plants) in the desert oasis (Table 2). The most significant difference generally occurred between phyllosphere and other soil locations (top or subsoil, independent of being with or without plants) (Table 2) with amounts in the phyllosphere generally being double to up to two hundred times (for total phenol content) of the rest of soil. Analysis confirmed the high  $\text{Na}^+$  and  $\text{NO}_3^-$  content of the soil, particularly the soil trapped in the plant canopy (Fig. S9). Overall, the soils were very low in plant-available P (Table 2). The Olsen-P values (mean 1.8 mg P  $\text{kg}^{-1}$ ) were much lower than those recovered with an acetic acid extract (mean 30.3 mg P  $\text{kg}^{-1}$ ;  $P < 0.001$ ). Further, the results showed that acetic acid extractable P was much greater in the soil with plants in comparison to the unvegetated areas.

P sorption isotherms revealed that the soils under *D. spicata* and in the corresponding unvegetated areas had an extremely high capacity to bind P (Fig. S17). In contrast, the phyllosphere soil had a much lower capacity to bind P. This is exemplified in the average P buffer power ( $B_p$ ) in the aerial phyllosphere soil which was  $11.5 \pm 1.7$  while it was  $519 \pm 93$  in the soil under the plants. Rates of ammonification assessed using the anaerobic incubation assay showed no difference between planted and unplanted soils, however, large rates of net  $\text{NH}_4^+$  production were seen in the phyllosphere soil (Table 2).

#### 3.3.2. Pore morphology results from X-ray CT

X-ray CT imaging revealed that the highly cemented (0–5 cm) layer at the base of the plant pedestal had significant amounts of plant rhizome material passing through it (Fig. 2). The presence of the cemented layer under the plants strongly suggested that it has formed prior to plant establishment. Whilst the plant material was consistently orientated in the same vertical direction, there was a clear structural discontinuity with respect to soil pore space. The pore space of the specimens as a whole were generally quite porous (c. 20%) with an average pore size of around 1  $\text{mm}^2$  and a relatively homogeneous pore size distribution (Fig. S10). However, when assessed as high- and low-density regions, clear differences were observed. At the resolution used in this study (58  $\mu\text{m}$ ), the porosity in the high-density region (directly at the soil surface) was <1% compared to 16% in the underlying low-density areas (Table S3). While the average pore sizes for the different regions are similar (0.13 and 0.20  $\text{mm}^2$  respectively for high- and low-density regions), clear differences in the pore size distribution (and coefficient of uniformity,  $\text{PSD}_{cu}$ ) did occur with many more of the smaller sized pores in the low-density region (Fig. S10, Table S3). Root

**Table 1**  
Chemical composition of the different tissues in *Distichlis spicata*.

Element	<i>Distichlis spicata</i>				<i>Adesmia atacamensis</i>	<i>Prosopis tamarugo</i>	<i>Atriplex atacamensis</i>	P value
	Fresh leaves	Senesced leaves	Stems	Roots	Fresh leaves	Fresh leaves	Fresh leaves	
Macronutrients (mg g <sup>-1</sup> )								
C	37.5 ± 0.8 <sup>c</sup>	37.6 ± 0.6 <sup>c</sup>	43.7 ± 0.2 <sup>a</sup>	41.7 ± 2.4 <sup>ab</sup>	44.2 ± 1.3 <sup>a</sup>	44.5 ± 0.5 <sup>a</sup>	36.4 ± 0.6 <sup>c</sup>	***
N	1.11 ± 0.07 <sup>c</sup>	0.50 ± 0.02 <sup>e</sup>	0.67 ± 0.03 <sup>de</sup>	0.93 ± 0.05 <sup>cd</sup>	2.06 ± 0.20 <sup>b</sup>	2.87 ± 0.19 <sup>a</sup>	2.20 ± 0.13 <sup>b</sup>	***
Na	37.6 ± 7.0 <sup>a</sup>	20.3 ± 4.0 <sup>b</sup>	10.5 ± 1.9 <sup>bc</sup>	3.4 ± 1.0 <sup>c</sup>	1.4 ± 0.2 <sup>c</sup>	1.6 ± 0.3 <sup>c</sup>	42.0 ± 0.9 <sup>a</sup>	***
K	10.2 ± 0.7 <sup>b</sup>	6.1 ± 0.6 <sup>c</sup>	6.0 ± 0.7 <sup>c</sup>	5.0 ± 0.7 <sup>c</sup>	3.9 ± 0.4 <sup>c</sup>	7.1 ± 1.9 <sup>bc</sup>	17.7 ± 3.7 <sup>a</sup>	***
Mg	1.4 ± 0.1 <sup>a</sup>	1.4 ± 0.1 <sup>a</sup>	1.3 ± 0.1 <sup>a</sup>	1.2 ± 0.1 <sup>a</sup>	1.0 ± 0.0 <sup>b</sup>	1.3 ± 0.2 <sup>a</sup>	1.2 ± 0.0 <sup>a</sup>	**
Ca	5.0 ± 0.6 <sup>b</sup>	6.1 ± 0.5 <sup>b</sup>	5.2 ± 0.8 <sup>b</sup>	8.5 ± 3.6 <sup>b</sup>	5.6 ± 0.6 <sup>b</sup>	20.6 ± 9.1 <sup>a</sup>	5.4 ± 0.4 <sup>b</sup>	*
P	0.39 ± 0.04 <sup>b</sup>	0.11 ± 0.01 <sup>c</sup>	0.27 ± 0.06 <sup>bc</sup>	0.34 ± 0.05 <sup>bc</sup>	0.33 ± 0.04 <sup>bc</sup>	0.47 ± 0.21 <sup>b</sup>	0.93 ± 0.27 <sup>a</sup>	***
S	2.72 ± 0.25	4.60 ± 0.16	4.35 ± 0.56	5.44 ± 2.12	3.37 ± 0.34	6.34 ± 3.87	2.95 ± 0.22	NS
Cl	104.3 ± 19.6 <sup>a</sup>	50.8 ± 8.7 <sup>b</sup>	34.9 ± 8.8 <sup>bc</sup>	11.6 ± 0.9 <sup>c</sup>	11.8 ± 0.8 <sup>c</sup>	11.2 ± 1.6 <sup>c</sup>	58.6 ± 0.3 <sup>b</sup>	***
Micronutrients (µg g <sup>-1</sup> )								
Fe	1200 ± 184 <sup>c</sup>	2770 ± 310 <sup>a</sup>	2225 ± 449 <sup>ab</sup>	3103 ± 1875 <sup>c</sup>	1311 ± 170 <sup>c</sup>	1353 ± 159 <sup>bc</sup>	490 ± 23 <sup>c</sup>	***
Mn	135 ± 10 <sup>a</sup>	119 ± 9 <sup>ab</sup>	85 ± 17 <sup>abc</sup>	72 ± 28 <sup>bc</sup>	38 ± 4 <sup>c</sup>	103 ± 43 <sup>abc</sup>	131 ± 19 <sup>ab</sup>	*
Ni	23 ± 5 <sup>cd</sup>	25 ± 2 <sup>cd</sup>	55 ± 6 <sup>a</sup>	35 ± 7 <sup>bc</sup>	50 ± 3 <sup>ab</sup>	19 ± 5 <sup>cd</sup>	13 ± 4 <sup>d</sup>	***
Cu	38 ± 4 <sup>b</sup>	62 ± 4 <sup>a</sup>	20 ± 10 <sup>bcd</sup>	15 ± 2 <sup>cd</sup>	13 ± 2 <sup>cd</sup>	34 ± 14 <sup>bc</sup>	10 ± 1 <sup>d</sup>	***
Zn	21 ± 2 <sup>bc</sup>	37 ± 4 <sup>ab</sup>	38 ± 1 <sup>a</sup>	49 ± 9 <sup>a</sup>	49 ± 10 <sup>abc</sup>	46 ± 12 <sup>a</sup>	17 ± 2 <sup>c</sup>	*
Nutrient ratio								
C/N	34 ± 3 <sup>bc</sup>	77 ± 9 <sup>a</sup>	66 ± 5 <sup>a</sup>	45 ± 5 <sup>b</sup>	22 ± 2 <sup>cd</sup>	16 ± 1 <sup>d</sup>	17 ± 2 <sup>d</sup>	***
Stable Isotopes (‰)								
δ <sup>13</sup> C	-15.3 ± 0.2 <sup>c</sup>	-14.9 ± 0.2 <sup>bc</sup>	-13.2 ± 0.8 <sup>a</sup>	-14.1 ± 0.2 <sup>ab</sup>	-25.3 ± 0.8 <sup>e</sup>	-23.5 ± 0.5 <sup>d</sup>	-15.0 ± 0.4 <sup>bc</sup>	***
δ <sup>15</sup> N	21.7 ± 7.7 <sup>a</sup>	13.6 ± 0.5 <sup>ab</sup>	13.7 ± 2.8 <sup>ab</sup>	12.0 ± 2.8 <sup>b</sup>	5.8 ± 1.1 <sup>b</sup>	11.9 ± 0.1 <sup>ab</sup>	11.2 ± 0.7 <sup>b</sup>	**

The nutrient composition of three other plants found at the site is provided for comparison. Values represent means ± SEM,  $n = 5$  for *D. spicata* and  $n = 3$  for the other species. Different letters indicate significant differences between groups at the  $P < 0.05$  level. The  $P$  value ANOVA symbols \*, \*\* and \*\*\* indicate significant differences at the  $P < 0.05$ ,  $P < 0.01$  and  $P < 0.001$  level respectively, while NS indicates no significant difference ( $P > 0.05$ ).

**Table 2**  
Chemical composition of soils under *Distichlis spicata* and in adjacent areas with no plants present.

	Area with <i>D. spicata</i> plants						Area with no plants				P value
	Phyllosphere soil		Topsoil		Subsoil		Topsoil		Subsoil		
Sand (g kg <sup>-1</sup> )	539	±25	432	±51	435	±99	385	±105	298	±58	NS
Silt (g kg <sup>-1</sup> )	211	±18	316	±23	349	±79	422	±76	420	±46	NS
Clay (g kg <sup>-1</sup> )	174	±17	220	±28	203	±23	151	±30	230	±23	NS
Soluble salts (g kg <sup>-1</sup> ) <sup>1</sup>	77	±15 <sup>a</sup>	32	±10 <sup>bc</sup>	13	±2 <sup>c</sup>	43	±8 <sup>bc</sup>	52	±16 <sup>ab</sup>	**
CaCO <sub>3</sub> (g kg <sup>-1</sup> )	31	±1 <sup>ab</sup>	29	±3 <sup>b</sup>	32	±5 <sup>ab</sup>	49	±4 <sup>a</sup>	39	±7 <sup>ab</sup>	*
Moisture content (g kg <sup>-1</sup> )	29	±2 <sup>b</sup>	157	±7 <sup>a</sup>	184	±21 <sup>a</sup>	64	±18 <sup>b</sup>	67	±17 <sup>b</sup>	***
pH	7.73	±0.20 <sup>c</sup>	8.75	±0.13 <sup>ab</sup>	8.43	±0.08 <sup>b</sup>	8.70	±0.16 <sup>ab</sup>	9.01	±0.03 <sup>a</sup>	***
EC (mS cm <sup>-1</sup> )	45.9	±7.5 <sup>a</sup>	14.9	±5.2 <sup>bc</sup>	6.2	±0.6 <sup>c</sup>	21.9	±5.2 <sup>bc</sup>	24.8	±7.8 <sup>b</sup>	**
NH <sub>4</sub> <sup>+</sup> (mg N kg <sup>-1</sup> )	1.81	±0.59 <sup>a</sup>	0.90	±0.36 <sup>ab</sup>	0.29	±0.09 <sup>b</sup>	0.76	±0.22 <sup>b</sup>	0.33	±0.07 <sup>b</sup>	*
NO <sub>3</sub> <sup>-</sup> (g N kg <sup>-1</sup> )	1.51	±0.68	0.69	±0.23	0.22	±0.07	1.08	±0.17	1.06	±0.38	NS
Total phenols (mg kg <sup>-1</sup> )	282	±49 <sup>a</sup>	12.4	±6.9 <sup>b</sup>	1.44	±0.41 <sup>b</sup>	3.07	±0.81 <sup>b</sup>	1.71	±0.36 <sup>b</sup>	***
Extractable Na (g kg <sup>-1</sup> )	25.5	±5.4 <sup>a</sup>	10.4	±3.7 <sup>bc</sup>	3.4	±0.7 <sup>c</sup>	14.3	±3.2 <sup>abc</sup>	18.6	±6.0 <sup>ab</sup>	*
Extractable K (g kg <sup>-1</sup> )	1.26	±0.26 <sup>a</sup>	0.51	±0.17 <sup>b</sup>	0.25	±0.03 <sup>b</sup>	0.31	±0.12 <sup>b</sup>	0.34	±0.06 <sup>b</sup>	***
Extractable Ca (g kg <sup>-1</sup> )	2.67	±0.30 <sup>a</sup>	1.30	±0.14 <sup>b</sup>	1.07	±0.04 <sup>b</sup>	1.66	±0.13 <sup>b</sup>	1.35	±0.11 <sup>b</sup>	***
Olsen available-P (mg kg <sup>-1</sup> )	3.58	±1.37 <sup>b</sup>	0.91	±0.42 <sup>a</sup>	0.97	±0.44 <sup>a</sup>	1.78	±0.35 <sup>ab</sup>	1.87	±0.53 <sup>ab</sup>	*
Acetic acid available P (mg kg <sup>-1</sup> )	23.4	±3.2 <sup>b</sup>	44.4	±6.4 <sup>a</sup>	48.3	±8.2 <sup>a</sup>	15.2	±2.7 <sup>b</sup>	20.0	±7.2 <sup>b</sup>	**
Dissolved organic C (mg kg <sup>-1</sup> )	7086	±1250 <sup>a</sup>	85	±43 <sup>b</sup>	13	±5 <sup>b</sup>	33	±7 <sup>b</sup>	20	±4 <sup>b</sup>	***
Total C (g kg <sup>-1</sup> )	1.07	±0.11 <sup>a</sup>	0.21	±0.04 <sup>b</sup>	0.16	±0.03 <sup>b</sup>	0.14	±0.03 <sup>b</sup>	0.18	±0.03 <sup>b</sup>	***
Total N (mg kg <sup>-1</sup> )	137	±33 <sup>a</sup>	64	±6 <sup>b</sup>	55	±11 <sup>b</sup>	101	±14 <sup>ab</sup>	97	±15 <sup>ab</sup>	*
Total soil C:N ratio	9.6	±2.1 <sup>a</sup>	3.3	±0.7 <sup>b</sup>	3.2	±0.6 <sup>b</sup>	1.4	±0.2 <sup>b</sup>	2.0	±0.4 <sup>b</sup>	***
Soil solution C:N ratio	7.51	±2.56 <sup>a</sup>	0.16	±0.12 <sup>b</sup>	0.07	±0.04 <sup>b</sup>	0.03	±0.01 <sup>b</sup>	0.03	±0.01 <sup>b</sup>	***
Ammonification rate (mg N kg <sup>-1</sup> d <sup>-1</sup> )	6.41	±2.12 <sup>a</sup>	0.58	±0.24 <sup>b</sup>	0.36	±0.07 <sup>b</sup>	0.59	±0.20 <sup>b</sup>	0.34	±0.09 <sup>b</sup>	***

Values represent means ± SEM,  $n = 5$ . Different letters indicate significant differences between treatments at the  $P < 0.05$  level. Where appropriate, all values are expressed on a dry weight basis. The  $P$  value ANOVA symbols \*, \*\* and \*\*\* indicate significant differences at the  $P < 0.05$ ,  $P < 0.01$  and  $P < 0.001$  level respectively, while NS indicates no significant difference ( $P > 0.05$ ).

material was clearly visible in both low- and high-density regions and showed large amounts of aerenchyma present within the tissue (Hansen et al., 1976; See Supplementary Movie S1 and Movie S2).

### 3.3.3. Origin and amounts of soil C and N stocks

Soil trapped in the *D. spicata* phyllosphere contained ca. 5 times higher levels of organic C than the underlying soil which were generally very low in C ( $0.17 \pm 0.01$  g kg<sup>-1</sup>; Table 2). This trend was also reflected in the levels of dissolved organic C and extractable phenolics which were also much higher in the phyllosphere soil. Soils in areas with and without plants contained comparable amounts of organic C in the top-

and underlying subsoil (Table 3). However, in the unvegetated area only 9–17% of the C was present as C<sub>4</sub>-C and thus from recent plant C inputs. In contrast, in the areas with *Distichlis spicata* plants the values were much higher ranging from 57 to 60% (Table 3). On an area basis, most of the organic C present in the planted soils was found in the phyllosphere ( $1941 \pm 866$  g C m<sup>-2</sup>). It contained double the amount of C, although being only half the depth (10 cm) of the other sampled soil compartments (Fig. S7). Furthermore, in the phyllosphere soil the organic C stocks consisted of >85% of more recent C<sub>4</sub>-C plant derived inputs, with the remainder being non-recent C<sub>3</sub> (Table 3; Fig. S12).



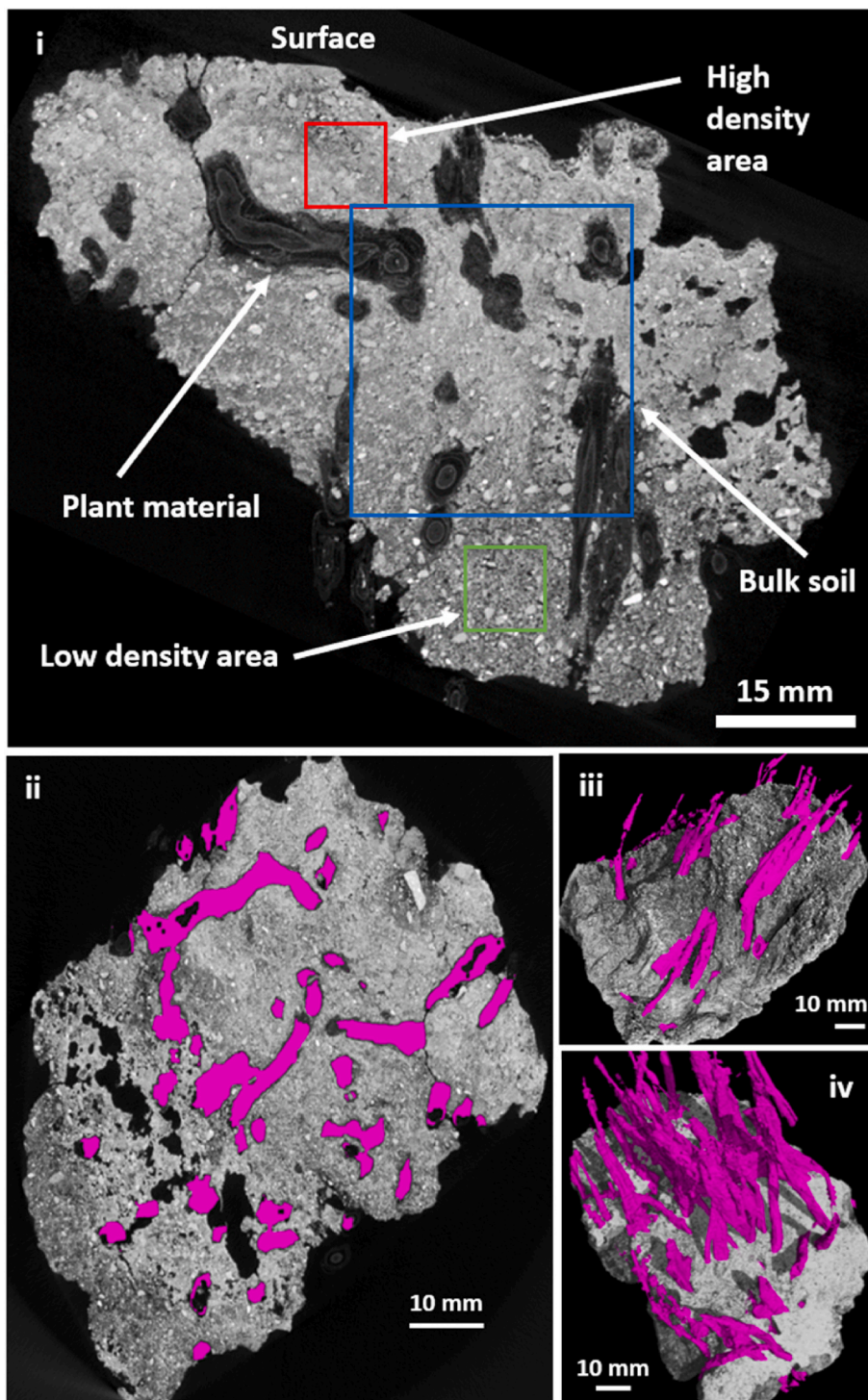


Fig. 2. X-ray scans of soil at the base (0–5 cm depth) of the *D. spicata* plant columns (i) showing the highly cemented (high density) region at the soil surface (sample area in red) and the underlying low-density matrix towards the top half (sample area in green) and the plant material (aerenchymous rhizomes) running through the soil. Bulk soil porosity analysis was performed on the largest possible sample area that could be accommodated due to the shape of the sample (highlighted in blue). (ii) Selected plant material highlighted in purple used as mask for analysis. (iii) 3D bulk volume representative image. (iv) 3D cross-sectional bulk volume showing the ingress of roots/organic matter into the sample.

### 3.4. Soil microbial communities

Overall, the size of the microbial biomass was 11-fold higher under the *D. spicata* plants in comparison to areas where no plants were present (Table 4). All other microbial parameters (i.e. Gram-negative and Gram-positive bacteria, fungi, putative arbuscular mycorrhizal fungi, actinomycetes) were also up to twenty-five times higher in the vegetated area (Table 4). With respect to soil depth, no differences were seen in either the size or structure of the microbial community in either the planted or unplanted areas. Based on the fatty acid profile, Gram-positive bacteria were present at much higher levels than Gram-negative bacteria (ca. 2-

fold higher;  $P < 0.001$ ), while fungal-specific or putative arbuscular mycorrhizal fungal fatty acid markers could only be detected under *D. spicata*. The soil trapped in the phyllosphere had a much lower microbial biomass, being comparable to that present in the unplanted areas (Table 4). In contrast to the unplanted top- and subsoils, the phyllosphere soil had a higher abundance of fungi (Table 4). While the fungal PLFA marker used here (18:2w6c) has previously been shown to be a reliable marker of fungal biomass (Frostegard and Bååth, 1996; Olsson, 1999; Kaiser et al., 2010), we cannot discount that some may also have originated from plant litter (Willers et al., 2015; Napier et al., 2014). Further qPCR, metabarcoding and metagenomic approaches should



**Table 3**

The carbon stocks of total soil organic C (SOC), recent ( $C_4$ -C) and older ( $C_3$ -C) in the soil compartment under *Distichlis spicata* or without plants (unvegetated).

Sample type	Soil <sup>13</sup> C (‰)	Amount of $C_4$ -C (% of total)	SOC (g C kg <sup>-1</sup> )	C stocks (g C m <sup>-2</sup> )	Recent $C_4$ -C (g C m <sup>-2</sup> )	Older $C_3$ -C (g C m <sup>-2</sup> )
Phyllosphere	-13.93 ± 1.02	86 ± 7	10.8 ± 2.41	1941 ± 866	1674	267
Topsoil (vegetated)	-17.58 ± 1.60	60 ± 11	2.08 ± 0.92	748 ± 330	450	298
Subsoil (vegetated)	-18.05 ± 1.27	57 ± 9	1.60 ± 0.62	575 ± 223	327	249
Topsoil (unvegetated)	-24.78 ± 0.50	9 ± 4	1.36 ± 0.56	491 ± 201	43	448
Subsoil (unvegetated)	-23.67 ± 1.65	17 ± 12	1.78 ± 0.56	642 ± 202	107	536

Values represent means ± SD or means only ( $n = 5$ ). The soil bulk density was assumed to be 1.8 g cm<sup>-3</sup>. Sampled soil depth interval were topsoil (0–20 cm) and subsoil (20–40 cm), except the phyllosphere soil for which only 10 cm was sampled from the plant column. The <sup>13</sup>C endmember plant  $C_4$  plant (100%) were set to -12‰ and  $C_3$  (100%) set to -26‰.

**Table 4**

Microbial biomass and the relative abundance of different microbial groups within the topsoil, subsoil and phyllosphere soil of *Distichlis spicata* in comparison to areas of bare ground where no plants are present.

	Area with <i>Distichlis spicata</i>			Area with no plants		P value
	Phyllosphere soil	Topsoil	Subsoil	Topsoil	Subsoil	
Microbial biomass (nmol g <sup>-1</sup> )	2.33 ± 1.03 <sup>b</sup>	10.7 ± 3.60 <sup>a</sup>	12.3 ± 3.44 <sup>a</sup>	1.37 ± 0.41 <sup>b</sup>	0.62 ± 0.29 <sup>b</sup>	**
Gram- bacteria (nmol g <sup>-1</sup> )	0.74 ± 0.38 <sup>bc</sup>	2.48 ± 1.20 <sup>a</sup>	3.34 ± 1.08 <sup>ab</sup>	0.49 ± 0.16 <sup>bc</sup>	0.16 ± 0.11 <sup>c</sup>	*
Gram + bacteria (nmol g <sup>-1</sup> )	1.38 ± 0.69 <sup>b</sup>	7.05 ± 2.19 <sup>a</sup>	8.03 ± 2.24 <sup>a</sup>	0.80 ± 0.23 <sup>b</sup>	0.43 ± 0.16 <sup>b</sup>	**
Putative AMF (nmol g <sup>-1</sup> )	<0.05	0.15 ± 0.01 <sup>a</sup>	0.19 ± 0.02 <sup>a</sup>	<0.05	<0.05	NS
Fungi (nmol g <sup>-1</sup> )	0.21 ± 0.08 <sup>a</sup>	0.48 ± 0.12 <sup>a</sup>	0.24 ± 0.06 <sup>a</sup>	<0.05	<0.05	NS
Actinomycetes (nmol g <sup>-1</sup> )	<0.05	0.52 ± 0.19 <sup>a</sup>	0.69 ± 0.19 <sup>a</sup>	0.08 ± 0.05 <sup>b</sup>	0.03 ± 0.02 <sup>b</sup>	**

Values represent means ± SEM,  $n = 5$ . Different superscript letters indicate significant differences between treatments at the  $P < 0.05$  level. The P value ANOVA symbols \*, \*\* and \*\*\* indicate significant differences at the  $P < 0.05$ ,  $P < 0.01$  and  $P < 0.001$  level respectively, while NS indicates no significant difference ( $P > 0.05$ ).

therefore be used to confirm this result.

### 3.5. Soil microbial activity and carbon and nitrogen mineralization

The microbial turnover of a low dose of glucose added to the soil (10 μM) is shown in Fig. 3. Overall, the rate of glucose turnover was very rapid in the soil under *D. spicata* relative to that in the bare soil devoid of plants ( $P < 0.001$ ). This is evidenced by the ca. 16-fold difference in mineralization rate between the two treatments in the first 24 h after substrate addition. In contrast to the soil trapped in the phyllosphere, the bare soil showed evidence of a lag phase in <sup>14</sup>CO<sub>2</sub> evolution which lasted for ca. 7 d after glucose addition. No significant difference in the rate of <sup>14</sup>CO<sub>2</sub> evolution was observed between the topsoil and subsoil under plants ( $P = 0.403$ ) with the same response also observed in the bare soil area ( $P = 0.841$ ). In contrast to the soil under the plants, the phyllosphere soil showed very little capacity to mineralize <sup>14</sup>C-glucose and exhibited a significant lag phase in <sup>14</sup>CO<sub>2</sub> evolution. At the end of the 48-d incubation period, only small amounts of <sup>14</sup>C-glucose could be recovered from the planted soil (2.1 ± 0.6%) or from the bare soil areas (8.5 ± 0.2%) with a NaCl extract, indicating that a large proportion of the <sup>14</sup>C had been immobilized in the microbial biomass. Our estimates suggest that the amount of glucose-C immobilized did not differ significantly in the below-ground treatments (48.5% of the total;  $P = 0.898$ ). In contrast, in the phyllosphere soil 80 ± 16% of the <sup>14</sup>C glucose remained in the soil after 48 d with only 12 ± 9% immobilized in the biomass.

The microbial response to the higher dose of glucose (10 mM) yielded similar patterns to that seen at the lower glucose dose, except that the proportionate rates of mineralization were much lower, and the lag phases were much longer (Fig. 4). In the rhizosphere soil the total amount of <sup>14</sup>CO<sub>2</sub> evolved was greater at the high glucose dose (64 ± 6%) in comparison to the low dose addition (48 ± 3%;  $P < 0.001$ ) and consequently the amount immobilized in the microbial biomass was lower (34 ± 6% versus 49 ± 3%, respectively;  $P < 0.001$ ). This led to significant differences in microbial C use efficiency (CUE) between the two glucose treatments in the soil under plants (Fig. 5). In contrast, no differences in CUE were seen in the soil without plants irrespective of soil depth or substrate concentration ( $P > 0.05$ ). No CUE values are

presented for the phyllosphere soil due to the large uncertainty associated with the data.

The mineralization of the <sup>14</sup>C-labelled plant litter is shown in Fig. 6. Overall, almost no mineralization of the plant material occurred over the 48-d incubation period in the phyllosphere soil. In contrast, significant breakdown was observed in the soil underlying the plants and to a lesser extent in the bare soil. Ten days after applying the plant litter, its rate of mineralization was 62-fold faster in the soils under plants relative to that in the bare soil or phyllosphere ( $P < 0.001$ ).

The turnover of <sup>14</sup>C-labelled arginine and the subsequent production of NH<sub>4</sub><sup>+</sup> and NH<sub>3</sub> is shown in Fig. 7. Following a similar pattern to glucose, the greatest rate of turnover was seen in the soil underlying the plants relative to the other treatments ( $P < 0.001$ ). The rate of N mineralization was closely coupled to the rate of C mineralization, being greater in the vegetated top- and sub-soil ( $r^2 = 0.84$ ;  $P = 0.012$ ; Fig. S15). Large amounts of NH<sub>3</sub> were emitted from the phyllosphere and bare soil areas, relative to the amount of NH<sub>4</sub><sup>+</sup> recovered at the end of the incubation period suggesting that most of the mineralized N was lost in a gaseous form (Fig. 7C). This contrasts with the rhizosphere soil where proportionally more of the arginine-derived N was retained as NH<sub>4</sub><sup>+</sup> relative to NH<sub>3</sub> ( $P < 0.023$ ). Despite this, a significant relationship was apparent between the rate of arginine-C mineralization and NH<sub>3</sub> production ( $r^2 = 0.86$ ; Fig. S16).

## 4. Discussion

### 4.1. Plant survival at the hyperarid climate extreme

Consistent with previous reports, we show that the hyperarid core of the Atacama Desert experiences large diurnal variations in air temperature and relative humidity (Azúa-Bustos et al., 2015). When combined with low amounts of rainfall, soil moisture, soil surface compaction, high salinity and nutrient imbalance it makes it a highly challenging environment for plants to survive (Marquet et al., 1998). The dominant plant, *D. spicata*, has a water efficient  $C_4$  metabolism, is hyper-salt tolerant (i.e. survival at >0.5 M NaCl) and can withstand temperatures of up to 57 °C (Golden et al., 1995; Warren and Brockelman, 1989; Lazarus et al., 2011). This halophytic trait is reflected in the high

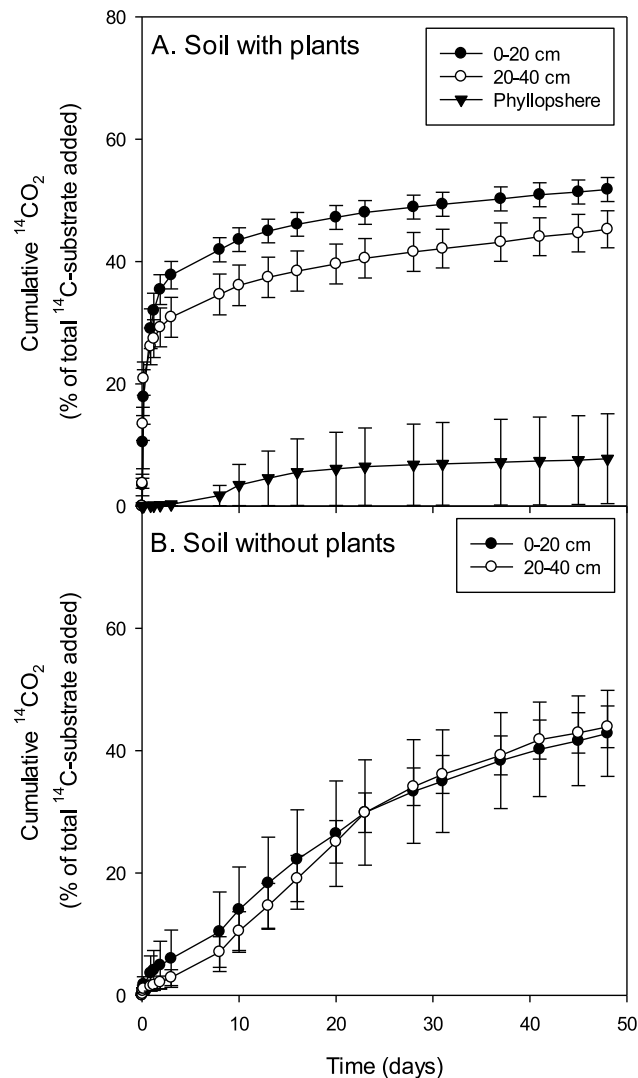


**Fig. 3.** Mineralization of a low concentration of <sup>14</sup>C-labelled glucose (10 μM) after addition to either (A) the phyllosphere soil, topsoil (0–20 cm) or subsoil (20–40 cm) associated with *D. spicata* plants or (B) in the corresponding areas of soil containing no plants. Values represent means ± SEM ( $n = 5$ ).

contents of NaCl in the leaves, the abundance of salt crystals on the leaf surface (Fig. S6b) and the presence of high amounts of salt in the phyllosphere soil. A comparison of salt in the vegetated and unvegetated soils suggests that *D. spicata* is effective at removing salt from the soil and discharging it into the above-ground component. For example, much lower levels of Na were seen in the roots relative to the shoots and in the subsoil relative to the phyllosphere soil. Our observations are also consistent with the excretion of Na via foliar salt glands in this plant (Semenova et al., 2010; Hasanuzzaman et al., 2014). Similar to Morris et al. (2019) we observed salt crystals on the leaf surface ranging in size from 25 to 100 μm in diameter. We speculate that these crystals will be blown off the leaf surface into the surrounding area (via the process of haloconduction; Yun et al., 2019), while other crystals become trapped within the phyllosphere soil. Based on the reduction of Na in soil under the plants, we estimate that the plants have effectively removed ca. 55% of the Na from the underlying soil, supporting the proposed use of halophytic salt shedding plants for land remediation purposes (Litalien et al., 2020).

As evidenced by the X-ray CT scans, the soil at the field site has an extremely hard and cemented surface horizon underlain by a more

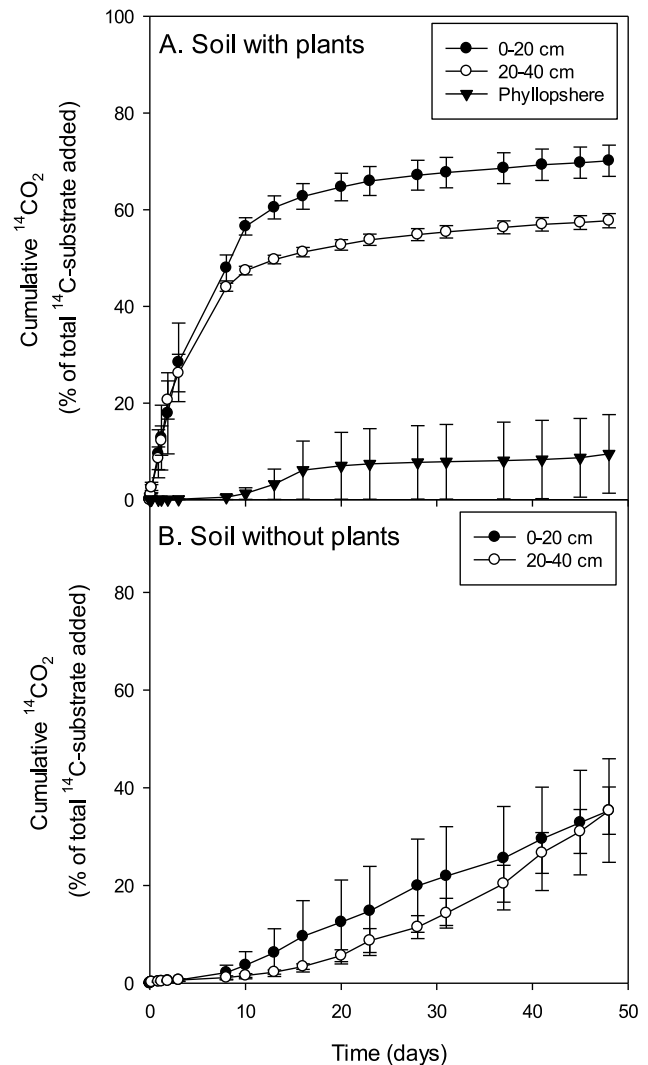


**Fig. 4.** Mineralization of a large concentration of <sup>14</sup>C-labelled glucose (10 mM) after addition to either (A) the phyllosphere, topsoil (0–20 cm) or subsoil (20–40 cm) associated with *D. spicata* plants or (B) in the corresponding areas of soil containing no plants. Values represent means ± SEM ( $n = 5$ ).

porous subsoil. We observed aerenchymous rhizomes of *D. spicata* with sharp points passing through this layer. After passage through this cemented layer there was a proliferation of secondary and tertiary roots. Our results are consistent with Hansen et al. (1976) who observed an abundance of epidermal silica cells which are thought to facilitate passage through highly compacted soil. These rhizomes are also likely to facilitate clonal growth and lateral plant establishment observed at the field site (Brewer and Bertness, 1996). The highly cemented layer is likely to restrict air movement into the soil (Weiler, 2005). Although we did not test this directly, the presence of large amounts of aerenchyma tissue in the vertical rhizomes passing through the cemented layer would support this (Colmer and Flowers, 2008).

#### 4.2. Soil moisture in the hyperarid core of the Atacama Desert

We observed that soil moisture was higher in the vegetated areas in comparison to unvegetated areas, the latter being similar to those reported previously (Fuentes et al., 2022a). Although the origin of this water was not investigated, we speculate that *D. spicata*, which is known to be deep rooting, employs hydraulic lift to bring up groundwater and redistribute it into the upper soil layers to promote microbial activity,

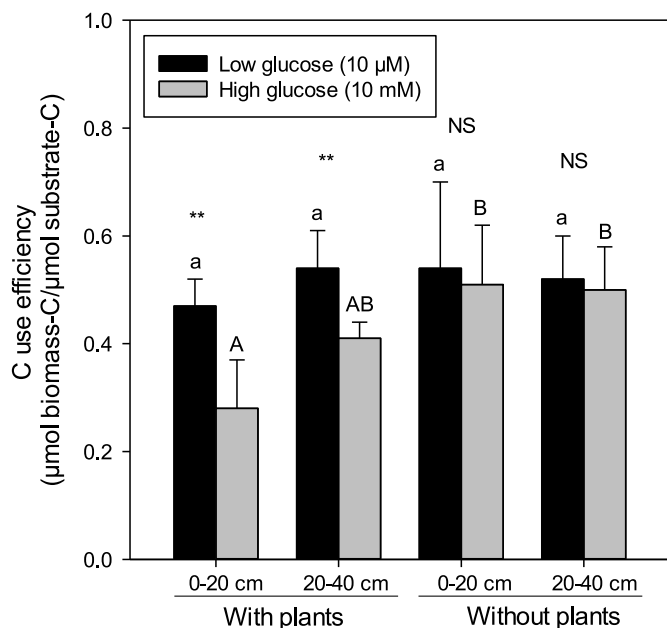


**Fig. 5.** Microbial carbon use efficiency (CUE) in either topsoil (0–20 cm) or subsoil (20–40 cm) in the presence or absence of plants (*D. spicata*) after the addition of a high (10 mM) or low (10  $\mu\text{M}$ ) dose of glucose to the soil. Values represent means  $\pm$  SEM ( $n = 5$ ). Different lowercase and uppercase letters represent significant differences between soils for the low and high glucose dose respectively ( $P < 0.05$ ). NS and \*\* indicate differences of either  $P > 0.05$  or  $P < 0.01$  between the high and low glucose doses for individual soils.

nutrient uptake and Na detoxification (Dawson, 1993; Armas et al., 2010). As the intrinsic moisture content in the phyllosphere soil was extremely low, we conclude that there is no evidence for hydraulic lift in this plant-soil compartment. Further work looking at the salinity and isotopic signature of the groundwater and constraints to water, however, are still needed (Bazihizina et al., 2017). The columnar structure growth form is uncommon for *D. spicata*, which typically grows low to the ground (Hansen et al., 1976). We speculate that columnar growth may confer some advantages for water conservation in the hyperarid core including: (i) provision of a windbreak, (ii) offering a large surface area for the condensation of fog water, (iii) lowering air and soil temperatures, all of which would decrease evaporation, positively affecting the soil moisture balance (Fuentes et al., 2022b; Sotomayor and Drezner, 2019). This is supported by previous studies showing that other plants in the Atacama Desert actively manage their micro-environment and moderate soil conditions, particularly on the driest and hottest days (Sotomayor and Drezner, 2019).

#### 4.3. Size and structure of the microbial community in hyperarid soils

As expected, the size of the soil microbial community was greatly enhanced in the presence of plants leading to the creation of biological hotspots within the hyperarid core of the Atacama Desert. Due to the cemented layer preventing leaf litter entering the soil, we ascribe this stimulation of microbial biomass and activity entirely due to rhizodeposition (root exudation and root/mycorrhizal turnover), the plant-mediated reduction in salt and the greater abundance of soil water (Jones et al., 2009). Evidence for the presence of arbuscular mycorrhizal fungi (AMF) is provided by the sole detection of the putative AMF PLFA marker 16:1w5c in the soil under the plants, and its absence from soil collected from the phyllosphere and unvegetated areas. It is also supported by previous reports describing the strong colonization of *D. spicata* by AMF in saline soils (Allen and Cunningham, 1983; Eppley et al., 2009). The origin, diversity of AMF spores and their functional role in promoting plant growth in these hyperarid soils requires further

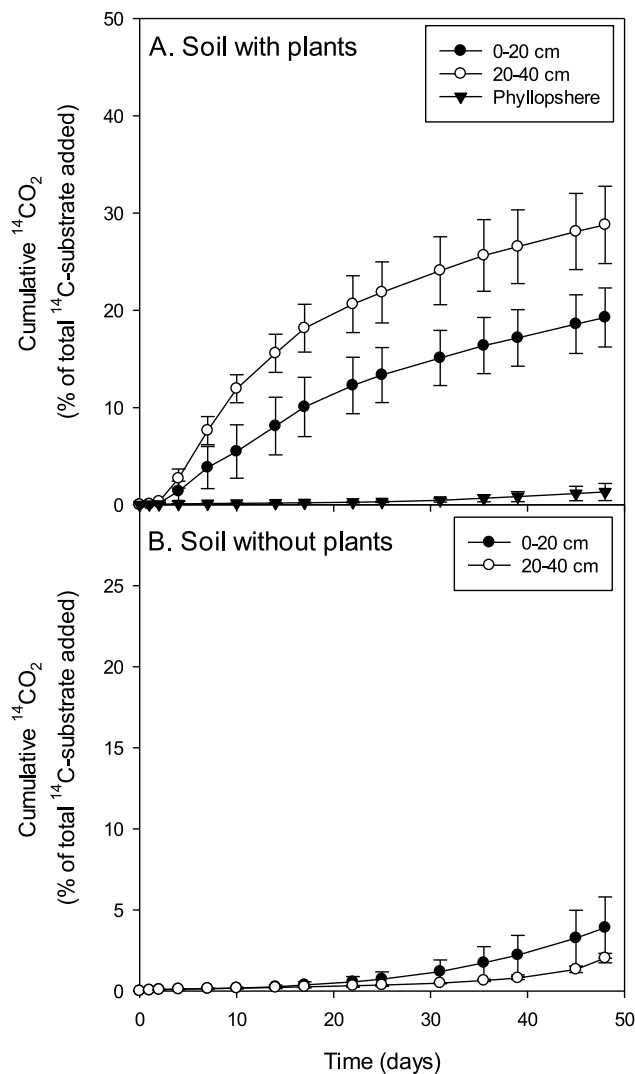


**Fig. 6.** Mineralization of  $^{14}\text{C}$ -labelled plant litter (10 mg  $\text{g}^{-1}$ ) after addition to either (A) the phyllosphere soil, underlying topsoil (0–20 cm) or subsoil (20–40 cm) associated with *D. spicata* plants or (B) in the corresponding areas of soil containing no plants. Values represent means  $\pm$  SEM ( $n = 5$ ).

investigation (i.e. nutrient and water uptake, stress tolerance), however, we assume that they are involved in promoting P acquisition given the low amounts and poor availability of P in our soils (Fig. S17). Interestingly, the presence of AMF appears to be related to the dioecious nature of *D. spicata* with differences in root colonization between male and female plants and that this difference in AMF may be linked to greater water use efficiency (Eppley et al., 2009; Reuss-Schmidt et al., 2015). Whether this sex trait links to plant performance in hyperarid climates and differences in growth forms is unknown and warrants further study.

In contrast to soils with no moisture limitation, all our samples showed a greater Gram-positive-to-Gram-negative ratio reflecting the adverse edaphic conditions and the prevalence of taxa viewed as being more stress tolerant and slower growing (Fanin et al., 2019; Chen et al., 2019). Of note, was the greater abundance of fungi in the phyllosphere soil, while it remained below the limit of detection in soil devoid of plants. The latter is in accordance with Kusch et al. (2020) and Shen (2020) who showed no evidence for an indigenous active fungal community in non-vegetated soils in the hyperarid core. The abundance of fungi in the phyllosphere soil, however, is supported by studies in non-hyperarid climates where leaves of *D. spicata* have been shown to

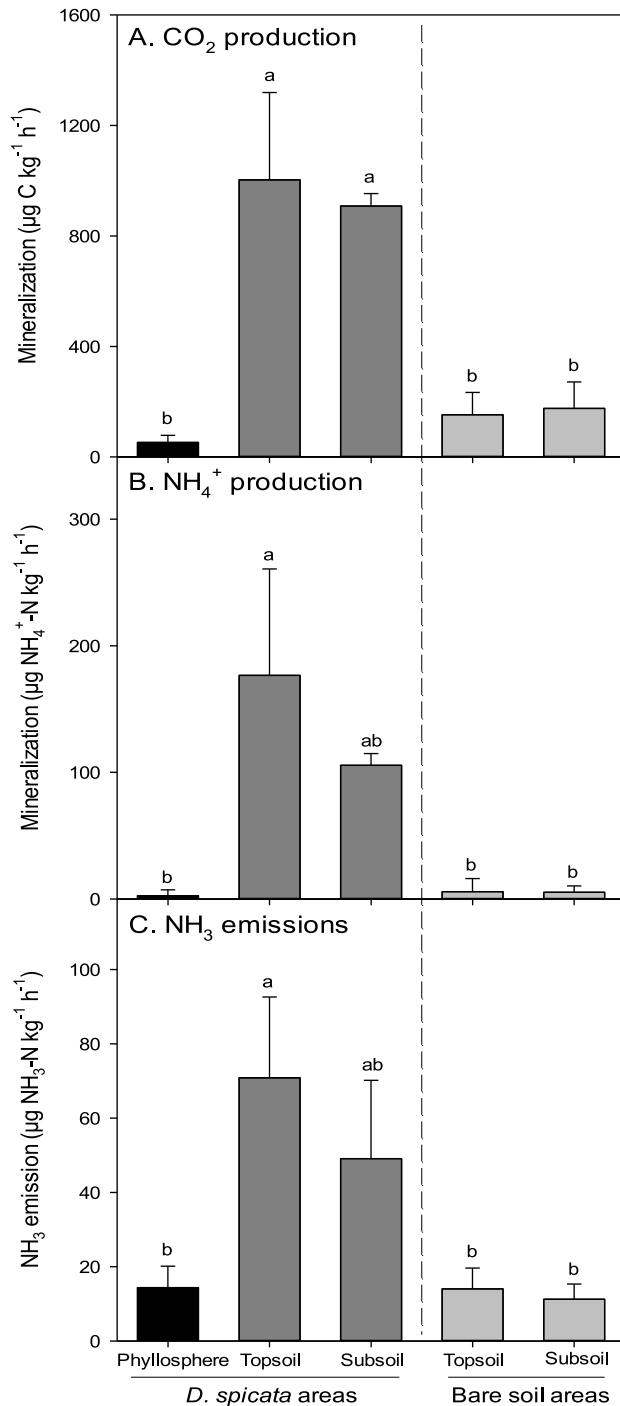


**Fig. 7.** Amount of <sup>14</sup>CO<sub>2</sub>, NH<sub>4</sub><sup>+</sup> and NH<sub>3</sub> produced after the addition of <sup>14</sup>C-labelled arginine to either the phyllosphere soil or underlying topsoil (0–20 cm) or subsoil (20–40 cm) associated with *D. spicata* plants or in the corresponding areas of soil containing no plants. Values represent means ± SEM (n = 5). Different letters represent significant differences between soils. The dotted line denotes the division between soils with and without plants.

harbour a wide diversity of fungi involved in the turnover of senescent leaf litter (Eliades et al., 2007; Calabon et al., 2021). Low levels of actinomycetes were detected in all samples, broadly in agreement with Okoro et al. (2009) who were able to recover significant numbers and diversity of these microorganisms in the Atacama Desert. Clearly, further work is required to further investigate the diversity of the active

microbial and mesofaunal communities within these environments. A caveat in our study is associated with the preservation of relic DNA and phospholipids in these soils (i.e., necromass) which may lead to an overestimate of microbial biomass size (Wilhelm et al., 2017; Shen, 2020). It should be clarified, however, that studies on the rate of phospholipid turnover in these soils is lacking and future work is needed to investigate the turnover of biomarkers in hyper-arid soils. We note that no mesofauna were visibly present in any of the soils investigated.

#### 4.4. Soil organic carbon in the hyperarid core of the Atacama Desert

Hyperarid regions of the Atacama Desert generally have low amounts of organic C (SOC), typically ranging from 100 to 500 mg C kg<sup>-1</sup> (Fuentes et al., 2022a; Lester et al., 2007) and very low levels of labile organic C (0.2–73 mg C kg<sup>-1</sup>; Fletcher et al., 2012; Mörchen et al., 2019). Our data is consistent with this showing similarly low levels of organic C (140–210 mg C kg<sup>-1</sup>) in both vegetated and non-vegetated areas. This suggests that either (i) rates of below-ground organic matter production are very low, (ii) that SOC turnover rates are very high under *D. spicata*, or (iii) that the site has not been vegetated for a long period of time, limiting the net accrual of SOC. It should be noted that these factors are not mutually exclusive with evidence available to support each of them. The biological hotspot studied here is associated with a surface aquifer and on rare occasions ephemeral rivers. It is possible that the older saltpetre or nitrate mines located in the study region (operating between 1880 and 1920) may have altered the hydrological balance and groundwater level present making it recently suited to plant establishment.

The δ<sup>13</sup>C values in the phyllosphere (-13.9‰), other soils under plants (-17.6 to -18.1‰) and bare soils devoid of plants (-24.8 to -23.7‰) are significantly different, but without differences between the top- and subsoils (Table 2). These results are in accordance with the recent study of Knief et al. (2020) reporting δ<sup>13</sup>C values of SOC between -22.7 and -28.0‰ in a hyper-aridity gradient of the Atacama Desert showing soil surface δ<sup>13</sup>C values for Yungay of -26.2 to -26.9‰. Ewing et al. (2008) did show that soil SOC δ<sup>13</sup>C ranged from -22.7 and -27.8‰ between 1 and 216 cm depth. These authors also suggest that in hyperarid soils, SOC is not a direct function of *in situ* photosynthesis but rather a result of atmospheric deposition of organic C (i.e. that C may therefore originate from outside the Atacama Desert region; see Arenas-Díaz et al., 2022).

If, we set the bare soil C<sub>4</sub> contribution of 9–17% as control (Table 3) and assume that the higher relative amount of C<sub>4</sub>-C in the vegetated soils (57–60%) and phyllosphere (>85%) are derived from *D. spicata* post-1920, we estimate an annual C turnover rate of 4.1, 2.2, and 15.9 g C m<sup>-2</sup> yr<sup>-1</sup> occurring in these top, surface and phyllosphere of the vegetated soils during the last 100 years. In terms of the turnover of C of the current C stocks, we would be looking for a steady state at turnover times of ~180, ~260–120 y for surface, subsurface and phyllosphere soil with plants. Warren-Rhodes et al. (2003) reported values of >600 y for active organic C cycling by hypolithic communities in wetter sites within the Atacama Desert, increasing to > 3000 y in the driest parts. Ziolkowski et al. (2013) suggested rate of C cycling for endolithic microbial communities in the hyperarid Core of the Atacama Desert to range from decadal to a millennium, the latter at the driest sampled site which was Yungay. Boutton et al. (1998) showed in semi-arid savanna ecosystems, that the mean residence time of SOC increased from ca. 40–100 y in the 0–15 cm depth interval, to ca. 300–500 y in the 15–30 cm interval. The bare soils devoid of plants possessed an ‘older’ C reservoir being mainly derived from C<sub>3</sub> plants, which were present in the past more humid times or originate from long-term atmospheric inputs being conserved in the soil (Ewing et al., 2006, 2008).

Total and dissolved organic C alongside phenolic substances were significantly higher in the phyllosphere soil relative to the other soil samples. This was expected as phenolic compounds are frequently produced by plants in response to oxidative stress and high salinity (Lopes



et al., 2021; Morales-Tapia et al., 2021; Zhang et al., 2022). In addition, the low intrinsic levels of microbial activity and physical protection against UV irradiation may have enhanced their persistence in this soil component. The high levels of phenolics may also have suppressed exoenzyme activity and thus microbial activity (Holik et al., 2017). This is evidenced by near-intact plant litter being found in the phyllosphere soil (Fig. S9). Our data on N availability in the phyllosphere soil also suggest that decomposition is not N limited, despite the high C-to-N ratio of the plant litter.

#### 4.5. Microbial processing of organic C in the hyperarid core of the Atacama desert

The highest rates of substrate-C mineralization were observed in the soil under plants, presumably due to the higher intrinsic microbial biomass, moisture content and reduced salinity (Jones et al., 2018a,b). It is also likely that a greater proportion of the microbial community was active due to the recent addition of C via rhizodeposition (Pathak and Rao, 1998). This is supported by the much higher mineralization rates in the vegetated topsoil when expressed on a microbial biomass basis. The mineralization data also indicated that small addition of substrate (10  $\mu\text{M}$  glucose), designed to reflect natural concentrations in the rhizosphere from root exudation (Jones et al., 2009), were rapidly utilized by the microbial community. Using a double exponential kinetic modelling approach to describe substrate turnover (Glanville et al., 2016), we estimate that the half-life of  $^{14}\text{C}$ -glucose in soil under the vegetated plants was short and ranged from 2 to 11 h (Table S5), albeit much slower than in temperate soils (Glanville et al., 2016; Hill et al., 2008). A similar calculation was not possible for the bare soils due to the poor model fit, probably reflecting the lag phase in mineralization reflecting the activation and/or growth of the microbial community. As expected, higher concentrations of glucose were mineralized much more slowly. This was particularly apparent in the bare soils where the very long lag phase suggested that the microbial community was too small to process the available-C or that there were insufficient other resources (e.g., P) to facilitate assimilation. Surprisingly, very low rates of microbial activity were observed in the phyllosphere soil with some samples exhibiting almost no measurable microbial activity. We ascribe this to the origin of the soil material which we believe is predominantly windblown and captured in the plant canopy. This process may be enhanced under high humidity conditions (i.e. fogs) which dissolve the salt crystals and make them conducive to soil binding (data not presented). While on the soil surface prior to transportation, this windblown material is likely to have experienced intense UV irradiation and temperature extremes, effectively sterilizing the material. It should be noted, however, that radio-resistant bacteria have been identified in desert sands from other regions of the world suggesting that they may also be present in the Atacama Desert (An et al., 2013; Liu et al., 2022). Our results also suggests that a large proportion of the PLFAs observed in the phyllosphere soil may not reflect an active microbial population but moreover preserved necromass. Further studies using stable isotope probing or transcriptomics should therefore be used to better elucidate the active microbial fraction in these soils. Our studies with plant litter clearly indicate that complex substrates are broken down much more slowly than simple C metabolites such as glucose. This suggests that the presence of microbial ectoenzymes and the subsequent breakdown of complex polymers (e.g., cellulose, protein) into readily assimilable oligomer units represents the rate limiting step in C turnover in these soils (Jones et al., 2018a,b).

Generally, the values for microbial CUE were relatively similar between the vegetated and unvegetated soils and for the low and high doses of glucose (CUE = 0.30–0.55). However, the values were much lower than reported for other parts of the world using the same glucose concentration (CUE = 0.55–0.75; Jones et al., 2018a,b). This indicates that the hyperarid microbial community is allocating less C towards cell maintenance and the generation of new biomass, but rather partitioning C into more energy intensive processes. We hypothesize that this will be

associated with the creation of osmoprotectants, operation of efflux pumps, the need to reduce  $\text{NO}_3^-$  to  $\text{NH}_4^+$  to acquire N, and processes associated with acquiring P from soil (e.g., release of phosphatases, organic acids) (Miller and Wood, 1996; Meng et al., 2018; Ameen et al., 2019). This allocation to catabolic processes was greatest in the vegetated soil when supplied with a large amount of glucose-C indicating that microbial growth appears to be inefficient in these hyperarid soils.

#### 4.6. Nitrogen and phosphorus cycling in the hyperarid core of the Atacama desert

Due to the extremely high  $\text{NO}_3^-$  concentrations in our soils ( $1.0 \pm 0.2 \text{ kg kg}^{-1}$ ;  $>2 \text{ t N ha}^{-1}$ ) we assume that N availability is not limiting microbial activity, rather it is the availability of labile C to firstly reduce  $\text{NO}_3^-$  to  $\text{NH}_4^+$  and the subsequent incorporation of this into organic N compounds (Schaeffer et al., 2003). N cycling will also be limited by the lack of available water and possibly P (Ewing et al., 2008; Jones et al., 2018a,b; Wu et al., 2021). Our findings are consistent with the accumulation of  $\text{NO}_3^-$  deposits on the soil surface under prolonged hyperarid conditions (Böhlike et al., 1997; Liu et al., 2017). We speculate that the higher amounts of  $\text{NO}_3^-$  present in the phyllosphere soil are a result of windblown accumulation of  $\text{NaNO}_3$ , as there is no evidence that *D. spicata* or any other plant to our knowledge can actively excrete  $\text{NO}_3^-$  from its leaves. Our analysis of the salt crystals on the leaf surface also showed no evidence for the presence of  $\text{NO}_3^-$  (data not shown). Comparison of the fresh and senesced leaves suggests a N, P and K re-assimilation rate of 55, 40 and 72%, respectively, suggesting tight nutrient cycling within the plant, especially for P which is low in the soils examined here (Aerts, 1996). It should be noted that the buffer power ( $B_p$ ) values for the non-phyllosphere soils are very high, supporting our measurements of very low bioavailability of P in soil (McDowell et al., 2023). We ascribe this to the strong association of P with minerals such as  $\text{CaSO}_4$  and the formation of poorly soluble Ca-P minerals, combined with the strongly alkaline soil pH (Guidry and Mackenzie, 2003; Shen et al., 2020). However, our results also suggest that the presence of plants is leading to a change in the size of the bioavailable P pools as evidenced by a depletion of the Olsen-P pool and a large net accumulation of P in the acid soluble pool. The latter P pool is likely to be recoverable by plants via organic acid exudation (Jones et al., 2009)

To our knowledge this is the first report of  $\text{NH}_3$  emissions occurring during the microbial processing of organic-N in the Atacama Desert. This represents another potential N loss pathway alongside denitrification (Wu et al., 2021). We ascribe this response to the low C:N ratio of arginine which drives microbial ammonification. After microbial uptake, a significant proportion of the arginine-derived C is used in catabolic processes with the excess  $\text{NH}_4^+$  excreted back into the soil, where the high pH subsequently promotes  $\text{NH}_3$  volatilization. This production of  $\text{NH}_3$ , however, may benefit other organisms with the capability to scavenge  $\text{NH}_3$  from the soil atmosphere (Lynch et al., 2014).

The  $\delta^{15}\text{N}$  in the phyllosphere was significantly higher (10.0‰) than in the soil samples (7.0–7.7‰). Similar soil  $\delta^{15}\text{N}$  values were reported by Díaz et al. (2016), especially for their most hyperarid sites (9.8–10.2‰). These authors suggested different mechanisms to explain these high positive  $\delta^{15}\text{N}$  values in these dry sites, including high N volatilization during elevated diurnal temperatures associated with very alkaline soils or formation of large pools of inorganic N as nitrate.

## 5. Conclusions

The Atacama Desert represents one of the most extreme places for life to establish on the planet. Within this study, we highlight the extreme climatic and edaphic conditions that exist in the hyperarid core of the Atacama Desert and how these might constrain life within the region. Despite these limitations, however, we demonstrate how the plant *D. spicata* has overcome these to promote plant establishment

within the region. Specifically, *D. spicata* appears to physically, chemically and biologically reengineer the system to relieve edaphic and climate stresses. Further, we demonstrate that *D. spicata* accelerates biogeochemical cycling. We also identify that the conversion of  $\text{NH}_4^+$  to  $\text{NH}_3$  during organic N turnover may represent a major N loss pathway within these desert ecosystems. In contrast to most ecosystems which are N limited, we show that microbial activity is not constrained by N, but rather by the availability of C and P. Despite the presence of plants, the net gain of soil organic C appears very low, suggesting that C turnover in these biological hotspots is high. In this context, further work is also required to better understand the active component of the rhizosphere microbial community and its functional role in promoting plant success. For example, numerous plant and microbial strategies exist to make P more bioavailable in soil (e.g. mycorrhizas, phosphatases,  $\text{H}^+$  and organic acid anion release, increased root hair density, transporter upregulation; Lambers, 2022), however, the relative importance of these and co-benefits for acquisition of water and other nutrients in hyperarid soil remains unknown and should be the subject of future study. In this study we used PLFAs to measure the size and structure of the soil microbial community, however, as noted above, this approach has its drawbacks and provides no information on key microbial taxa which may be influenced by *D. spicata* (e.g. mesofauna, archaea etc). It would therefore be desirable to combine the use of  $^{13}\text{C}$ -labelled substrates and compound-specific isotope ratio mass spectrometry (IRMS) to detect which PLFA-taxa were most enriched and therefore of greatest functional significance in carbon turnover (Broughton et al., 2015). Similarly, metagenomic approaches, metabarcoding and  $^{18}\text{O}$  labelling may provide insights at a much deeper taxonomic level (Morris et al., 2022). The work undertaken here on  $\text{NH}_3$  emissions showed the potential for N to be lost from soil, however, it would be desirable to measure this in the field. Lastly, perchlorates ( $\text{ClO}_4^-$ ) and iodates ( $\text{IO}_3^-$ ) are often present in high concentrations in soils from the Atacama Desert (Catling et al., 2010; Calderon et al., 2014; Lybrand et al., 2016), however, their role in regulating biological activity and biogeochemical cycling remains largely unknown. Further work should therefore focus on potential plant and microbial adaptive strategies to coping with these oxyanions and their potential for abiotic catalysis of C turnover.

The hyperarid soils of the Atacama Desert are often used as an analogue of the soils/regolith which might occur on Mars and exoplanets (Navarro-Gonzalez et al., 2003; Azúa-Bustos et al., 2022). However, evidence suggests that the soils of Mars are composed largely of volcanic basaltic rocks, fine dust, and a variety of mineral oxides and are rich in Fe and Mg, while those of the Atacama Desert are primarily composed of weathered rocks, sand, clay, and salts. In addition, the surface of Mars is subject to greater extremes in temperature, higher levels of radiation and low atmospheric pressure (Galletta et al., 2007, 2009). It would be desirable to investigate how organisms present in our hyperarid Atacama Desert soils respond to conditions which simulate the surface of Mars. Similarly, *D. spicata* may be a good model higher plant to investigate the potential for establishing vegetation on Mars, potentially using replica Martian soils (Kral et al., 2004).

#### CRedit author statement

Conceptualization, DLJ, RB, FAD, BF; Methodology DLJ, FAD, RB, RvH, BSA; Investigation, DLJ, FAD, RvH, BSA; Resources BSA, SJM, DLJ, FAD; Data Curation, DLJ, RvH, FAD; Writing – Original Draft, DLJ; Writing - Review & Editing, BF, FAD, DLJ, FR, SJM, RB; Supervision, BF, FR, RB; Funding acquisition, DLJ, BF, FR, RB.

#### Declaration of competing interest

The authors declare the following financial interests/personal relationships which may be considered as potential competing interests: Davey Jones reports financial support was provided by Biotechnology and Biological Sciences Research Council. Roland Bol reports financial

support was provided by German Research Foundation. Barbara Fuentes reports financial support was provided by National Agency for Research and Development. Francisco Remonsellez reports financial support was provided by National Agency for Research and Development. Davey Jones reports financial support was provided by Natural Environment Research Council.

#### Data availability

Data will be made available on request.

#### Acknowledgements

This work was funded by the UK Biotechnology and Biological Sciences Research Council (BB/N013204/1), Chilean National Agency for Research and Development ANID-MEC-80190012 and ANID-FONDECYT-1220902 projects and the ABCJ Geoverbund, German Science Foundation (DFG) as part of CRC1211, Helmholtz Association grant 2173 “Toward a Sustainable Bioeconomy - Resources, Utilization, Engineering and Agroecosystems” (POF IV:2021–2026). We thank Francisco A. Gomez-Valenzuela for help in the field and Anna Ray and Emily Cooledge for help in running the laboratory experiments. We thank Sarah Eppley at Portland State University and James Richards at UC Davis for their insights on the morphology and genetics of *D. spicata*.

#### Appendix A. Supplementary data

Supplementary data to this article can be found online at <https://doi.org/10.1016/j.soilbio.2023.109128>.

#### References

- Aerts, R., 1996. Nutrient resorption from senescing leaves of perennials: are there general patterns? *Journal of Ecology* 84, 597–608. <https://doi.org/10.2307/2261481>.
- Alfaro, F.D., Manzano, M., Almiray, C., Garcia, J.L., Osses, P., del Rio, C., Vargas, C., Latorre, C., Koch, M.A., Siegmund, A., Abades, S., 2021. Soil bacterial community structure of fog-dependent *Tillandsia landbeckii* dunes in the Atacama Desert. *Plant Systematics and Evolution* 307, 56. <https://doi.org/10.1007/s00606-021-01781-0>.
- Allen, E.B., Cunningham, G.L., 1983. Effects of vesicular-arbuscular mycorrhizae on *Distichlis spicata* under three salinity levels. *New Phytologist* 93, 227–236. <https://doi.org/10.1111/j.1469-8137.1983.tb03427.x>.
- Ameen, F., AlYahya, S.A., AlNadhari, S., Alasmari, H., Alhoshani, F., Wainwright, M., 2019. Phosphate solubilizing bacteria and fungi in desert soils: species, limitations and mechanisms. *Archives of Agronomy and Soil Science* 65, 1446–1459. <https://doi.org/10.1080/03650340.2019.1566713>.
- Amundson, R., Dietrich, W., Bellugi, D., Ewing, S., Nishiizumi, K., Chong, G., Owen, J., Finkel, R., Heimsath, A.M., Stewart, B., Caffee, M., 2012. Geomorphologic evidence for the late Pliocene onset of hyperaridity in the Atacama Desert. *Bulletin of the Geological Society of America* 124, 1048–1070. <https://doi.org/10.1130/B30445.1>.
- An, S., Couteau, C., Luo, F., Neveu, J., DuBow, M.S., 2013. Bacterial diversity of surface sand samples from the Gobi and Taklamakan Deserts. *Microbial Ecology* 66, 850–860. <https://doi.org/10.1007/s00248-013-0276-2>.
- Araya, J.P., Gonzalez, M., Cardinale, M., Schnell, S., Stoll, A., 2020. Microbiome dynamics associated with the Atacama flowering desert. *Frontiers in Microbiology* 10, 3160. <https://doi.org/10.3389/fmicb.2019.03160>.
- Arenas-Díaz, F., Fuentes, B., Reyers, M., Fiedler, S., Böhm, C., Campos, E., Shao, Y., Bol, B., 2022. Dust and aerosols in the Atacama Desert. *Earth-Science Reviews* 226, 103925. <https://doi.org/10.1016/j.earscirev.2022.103925>.
- Armas, C., Padilla, F.M., Pugnaire, F.I., Jackson, R.B., 2010. Hydraulic lift and tolerance to salinity of semiarid species: consequences for species interactions. *Oecologia* 162, 11–21. <https://doi.org/10.1007/s00442-009-1447-1>.
- Arndt, H., Ritter, B., Rybarski, A., Schiwitz, S., Dunai, T., Nitsche, F., 2020. Mirroring the effect of geological evolution: protist divergence in the Atacama Desert. *Global and Planetary Change* 190, 103193. <https://doi.org/10.1016/j.gloplacha.2020.103193>.
- Azúa-Bustos, A., González-Silva, C., Mancilla, R.A., Salas, L., Gómez-Silva, B., McKay, C. P., Vicuña, R., 2011. Hypolithic cyanobacteria supported mainly by fog in the coastal range of the Atacama Desert. *Microbial Ecology* 61, 568–581. <https://doi.org/10.1007/s00248-010-9784-5>.
- Azúa-Bustos, A., Urrejola, C., Vicuña, R., 2012. Life at the dry edge: microorganisms of the Atacama Desert. *FEBS Letters* 586, 2939–2945. <https://doi.org/10.1016/j.febslet.2012.07.025>.
- Azúa-Bustos, A., Caro-Lara, L., Vicuña, R., 2015. Discovery and microbial content of the driest site of the hyper-arid Atacama Desert, Chile. *Environmental Microbiology Reports* 7, 388–394. <https://doi.org/10.1111/1758-2229.12261>.





- Jones, D.L., Nguyen, C., Finlay, R.D., 2009. Carbon flow in the rhizosphere: carbon trading at the soil-root interface. *Plant and Soil* 321, 5–33. <https://doi.org/10.1007/s11104-009-9925-0>.
- Jones, D.L., Olivera-Ardid, S., Klumpp, E., Knief, C., Hill, P.W., Lehdorff, E., Bol, R., 2018a. Moisture activation and carbon use efficiency of soil microbial communities along an aridity gradient in the Atacama Desert. *Soil Biology and Biochemistry* 117, 68–71. <https://doi.org/10.1016/j.soilbio.2017.10.026>.
- Jones, D.L., Hill, P.W., Smith, A.R., Farrell, M., Ge, T., Banning, N.C., Murphy, D.V., 2018b. Role of substrate supply on microbial carbon use efficiency and its role in interpreting soil microbial community-level physiological profiles (CLPP). *Soil Biology and Biochemistry* 123, 1–6. <https://doi.org/10.1016/j.soilbio.2018.04.014>.
- Jones, D.L., Rousk, J., Edwards-Jones, G., DeLuca, T.H., Murphy, D.V., 2012. Biochar-mediated changes in soil quality and plant growth in a three year field trial. *Soil Biology and Biochemistry* 45, 113–124. <https://doi.org/10.1016/j.soilbio.2011.10.012>.
- Kaiser, C., Frank, A., Wild, B., Koranda, M., Richter, A., 2010. Negligible contribution from roots to soil-borne phospholipid fatty acid fungal biomarkers 18:2 $\omega$ 6,9 and 18:1 $\omega$ 9. *Soil Biology and Biochemistry* 42, 1650–1652. <https://doi.org/10.1016/j.soilbio.2010.05.019>.
- Kemmitt, S.J., Wright, D., Goulding, K.W.T., Jones, D.L., 2006. pH regulation of carbon and nitrogen dynamics in two agricultural soils. *Soil Biology and Biochemistry* 38, 898–911. <https://doi.org/10.1016/j.soilbio.2005.08.006>.
- Kidron, G.J., 2009. The effect of shrub canopy upon surface temperatures and evaporation in the Negev Desert. *Earth Surface Processes and Landforms* 34, 123–132. <https://doi.org/10.1002/esp.1706>.
- Knief, C., Bol, R., Amelung, W., Kusch, S., Frindt, K., Eckmeier, E., Jaeschke, A., Dunai, T., Fuentes, B., Mörchen, R., Schütte, T., Lücke, A., Klumpp, E., Kaiser, K., Rethemeyer, J., 2020. Tracing elevational changes in microbial life and organic carbon sources in soils of the Atacama Desert. *Global and Planetary Change* 184, 103078. <https://doi.org/10.1016/j.gloplacha.2019.103078>.
- Kohn, M.J., 2010. Carbon isotope compositions of terrestrial C3 plants as indicators of (paleo) ecology and (paleo) climate. *Proceedings of the National Academy of Sciences* 107, 19691–19695. <https://doi.org/10.1073/pnas.1004933107>.
- Kral, T.A., Bekkum, C.R., McKay, C.P., 2004. Growth of methanogens on a Mars soil simulant. *Origins of Life and Evolution of the Biosphere* 34, 615–626. <https://doi.org/10.1023/b:orig.0000043129.68196.5f>.
- Kresović, M.M., Antić-Mladenović, B.S., Ličina, D.V., 2005. Aerobic and anaerobic incubation biological indexes of soil nitrogen availability. *Proceeding of the National Academy of Sciences, Matrica Srpska Novi Sad* 109, 45–57.
- Kusch, S., Jaeschke, A., Mörchen, R., Rethemeyer, J., 2020. Tracing life at the dry limit using phospholipid fatty acids - does sampling matter? *Soil Biology and Biochemistry* 141, 107661. <https://doi.org/10.1016/j.soilbio.2019.107661>.
- Lambers, H., 2022. Phosphorus acquisition and utilization in plants. *Annual Review of Plant Biology* 73, 17–42. <https://doi.org/10.1146/annurev-arplant-102720-125738>.
- Lazarus, B.E., Richards, J.H., Gordon, P.E., Oki, L.R., Barnes, C.S., 2011. Plasticity tradeoffs in salt tolerance mechanisms among desert *Distichlis spicata* genotypes. *Functional Plant Biology* 38, 187–198. <https://doi.org/10.1071/FP10192>.
- Lester, E.D., Satomi, M., Ponce, A., 2007. Microflora of extreme arid Atacama Desert soils. *Soil Biology and Biochemistry* 39, 704–708. <https://doi.org/10.1016/j.soilbio.2006.09.020>.
- Litalien, A.A., Raymond, W.D., Rutter, A., Zeeb, B.A., 2020. Development of a model for the dispersal of salts from recretahalophytes. *ACS Earth and Space Chemistry* 4, 1367–1374. <https://doi.org/10.1021/acsearthspacechem.0c00800>.
- Liu, D., Zhu, W., Wang, X., Pan, Y., Wang, C., Xi, D., Bai, E., Wang, Y., 2017. Abiotic versus biotic controls on soil nitrogen cycling in drylands along a 3200 km transect. *Biogeosciences* 14, 989–1001. <https://doi.org/10.5194/bg-14-989-2017>.
- Liu, Y., Chen, T., Li, J., Wu, M.H., Liu, G.X., Zhang, W., Zhang, B.L., Zhang, S.L., Zhang, G.S., 2022. High proportions of radiation-resistant strains in culturable bacteria from the Taklimakan Desert. *Biology* 11, 501. <https://doi.org/10.3390/biology11040501>.
- Liu, J.Q., Sun, X., Zuo, Y.L., Hu, Q.N., He, X.L., 2023. Plant species shape the bacterial communities on the phyllosphere in a hyper-arid desert. *Microbiological Research* 269, 127314. <https://doi.org/10.1016/j.micres.2023.127314>.
- Lopes, M., Sanches-Silva, A., Castilho, M., Cavaleiro, C., Ramos, F., 2021. Halophytes as source of bioactive phenolic compounds and their potential applications. *Critical Reviews in Food Science and Nutrition* 63, 1078–1101. <https://doi.org/10.1080/10408398.2021.1959295>.
- Lybrand, R.A., Bockheim, J.G., Ge, W.S., Graham, R.C., Hlohowskyj, S.R., Michalski, G., Prellwitz, J.S., Rech, J.A., Wang, F., Parker, D.R., 2016. Nitrate, perchlorate, and iodate co-occur in coastal and inland deserts on Earth. *Chemical Geology* 442, 174–186. <https://doi.org/10.1016/j.chemgeo.2016.05.023>.
- Lynch, R.C., Darcy, J.L., Kane, N.C., Nemergut, D.R., Schmidt, S.K., 2014. Metagenomic evidence for metabolism of trace atmospheric gases by high-elevation desert Actinobacteria. *Frontiers in Microbiology* 5, 698. <https://doi.org/10.3389/fmicb.2014.00698>.
- Marquet, P.A., Bozinovic, F., Bradshaw, G.A., Cornelius, C., Gonzalez, H., Gutierrez, J.R., Hajek, E.R., Lagos, J.A., Lopez-Cortes, F., Nunez, L., Rosello, E.F., Santoro, C., Samaniego, H., Standen, V.G., Torres-Mura, J.C., Jaksic, F.M., 1998. Ecosystems of the Atacama Desert and adjacent Andean area in northern Chile. *Revista Chilena de Historia Natural* 71, 593–617.
- McCray, J.M., Wright, A.L., Luo, Y.G., Ji, S.N., 2012. Soil phosphorus forms related to extractable phosphorus in the everglades agricultural area. *Soil Science* 177, 31–38. <https://doi.org/10.1097/SS.0b013e31823782da>.
- McDowell, R.W., Noble, A., Pletnyakov, P., Haygarth, P.M., 2023. A global database of soil plant available phosphorus. *Scientific Data* 10, 125. <https://doi.org/10.1038/s41597-023-02022-4>.
- McKay, C.P., Friedmann, E.I., Gómez-Silva, B., Cáceres-Villanueva, L., Andersen, D.T., Landheim, R., 2003. Temperature and moisture conditions for life in the extreme arid region of the Atacama Desert: four years of observations including the El Niño of 1997–1998. *Astrobiology* 3, 393–406. <https://doi.org/10.1089/153110703769016460>.
- Meng, Y.B., Yin, C.Q., Zhou, Z.B., Meng, F.G., 2018. Increased salinity triggers significant changes in the functional proteins of ANAMMOX bacteria within a biofilm community. *Chemosphere* 207, 655–664. <https://doi.org/10.1016/j.chemosphere.2018.05.076>.
- Miller, K.J., Wood, J.M., 1996. Osmoadaptation by rhizosphere bacteria. *Annual Review of Microbiology* 50, 101–136. <https://doi.org/10.1146/annurev.micro.50.1.101>.
- Mintz, Y., Walker, G.K., 1993. Global fields of soil moisture and land surface evapotranspiration derived from observed precipitation and surface air temperature. *Journal of Applied Meteorology* 32, 1305–1334. [https://doi.org/10.1175/1520-0450\(1993\)032<1305:GFOSMA>2.0.CO;2](https://doi.org/10.1175/1520-0450(1993)032<1305:GFOSMA>2.0.CO;2).
- Miranda, K.M., Espey, M.G., Wink, D.A., 2001. A rapid, simple spectrophotometric method for simultaneous detection of nitrate and nitrite. *Nitric Oxide Biology and Chemistry* 5, 62–71. <https://doi.org/10.1006/niox.2000.0319>.
- Morales-Tapia, P., Cabrera-Barjas, G., Giordano, A., 2021. Polyphenolic distribution in organs of *Argylia radiata*, an extremophile plant from Chilean Atacama desert. *Natural Product Research* 35, 4143–4147. <https://doi.org/10.1080/14786419.2020.1739678>.
- Mörchen, R., Lehdorff, E., Arenas-Díaz, F., Moradi, G., Bol, R., Fuentes, B., Klumpp, E., Amelung, W., 2019. Carbon accrual in the Atacama Desert. *Global and Planetary Change* 181, 102993. <https://doi.org/10.1016/j.gloplacha.2019.102993>.
- Morris, K.A., Richter, A., Migliavacca, M., Schrupf, M., 2022. Growth of soil microbes is not limited by the availability of nitrogen and phosphorus in a Mediterranean oak-savanna. *Soil Biology and Biochemistry* 169, 108680. <https://doi.org/10.1016/j.soilbio.2022.108680>.
- Morris, L., Yun, K., Rutter, A., Zeeb, B.A., 2019. Characterization of excreted salt from the recretahalophytes *Distichlis spicata* and *Spartina pectinata*. *Journal of Environmental Quality* 48, 1775–1780. <https://doi.org/10.2134/jeq2019.03.0102>.
- Mulvaney, R.L., 1996. Nitrogen- inorganic forms. In: Sparks, D.L. (Ed.), *Methods of Soil Analysis. Part3. Soil Society of America Inc., Madison, WI*, pp. 1123–1184.
- Murphy, J., Riley, J.P., 1962. A modified single solution method for the determination of phosphate in natural waters. *Analytica Chimica Acta* 27, 31–36. [https://doi.org/10.1016/S0003-2670\(00\)88444-5](https://doi.org/10.1016/S0003-2670(00)88444-5).
- Napier, J.A., Haslam, R.P., Beaudoin, F., Cahoon, E.B., 2014. Understanding and manipulating plant lipid composition: metabolic engineering leads the way. *Current Opinion in Plant Biology* 19, 68–75. <https://doi.org/10.1016/j.pbi.2014.04.001>.
- Navarro-Gonzalez, R., Rainey, F.A., Molina, P., Bagaley, D.R., Hollen, B.J., de la Rosa, J., Small, A.M., Quinn, R.C., Grunthaler, F.J., Cáceres, L., 2003. Mars-like soils in the Atacama Desert, Chile, and the dry limit of microbial life. *Science* 302, 1018–1021. <https://doi.org/10.1126/science.1089143>.
- Okoro, C.K., Brown, R., Jones, A.L., Andrews, B.A., Asenjo, J.A., Goodfellow, M., Bull, A.T., 2009. Diversity of culturable actinomycetes in hyper-arid soils of the Atacama Desert, Chile. *Antonie van Leeuwenhoek* 95, 121–133. <https://doi.org/10.1007/s10482-008-9295-2>.
- Olsson, P.A., 1999. Signature fatty acids provide tools for determination of the distribution and interactions of mycorrhizal fungi in soil. *FEMS Microbiology Ecology* 29, 303–310. <https://doi.org/10.1111/j.1574-6941.1999.tb00621.x>.
- Pathak, H., Rao, D.L.N., 1998. Carbon and nitrogen mineralization from added organic matter in saline and alkali soils. *Soil Biology and Biochemistry* 30, 695–702. [https://doi.org/10.1016/S0038-0717\(97\)00208-3](https://doi.org/10.1016/S0038-0717(97)00208-3).
- Pfeiffer, M., Morgan, A., Heimsath, A., Jordan, T., Howard, A., Amundson, R., 2021. Century scale rainfall in the absolute Atacama Desert: landscape response and implications for past and future rainfall. *Quaternary Science Reviews* 254, 106797. <https://doi.org/10.1016/j.quascirev.2021.106797>.
- Reuss-Schmidt, K., Rosenstiel, T.N., Rogers, S.R., Simpson, A.G., Eppley, S.M., 2015. Effects of sex and mycorrhizal fungi on gas exchange in the dioecious salt marsh grass *Distichlis spicata*. *International Journal of Plant Sciences* 176, 141–149. <https://doi.org/10.1086/679351>.
- Rondanelli, R., Molina, A., Falvey, M., 2015. The Atacama surface solar maximum. *Bulletin of the American Meteorological Society* 96, 405–418. <https://doi.org/10.1175/BAMS-D-13-00175.1>.
- Santander, C., Garcia, S., Moreira, J., Aponte, H., Araneda, P., Olave, J., Vidal, G., Cornejo, P., 2021. Arbuscular mycorrhizal fungal abundance in elevation belts of the hyperarid Atacama Desert. *Fungal Ecology* 51, 101060. <https://doi.org/10.1016/j.funeco.2021.101060>.
- Semenova, G.A., Fomina, I.R., Biel, K.Y., 2010. Structural features of the salt glands of the leaf of *Distichlis spicata* 'Yensen 4a' (Poaceae). *Protoplasma* 240, 75–82. <https://doi.org/10.1007/s00709-009-0092-1>.
- She, W.W., Chen, N., Zhang, Y.Q., Qin, S.G., Bai, Y.X., Feng, W., Lai, Z.R., Qiao, Y.G., Liu, L., Zhang, W.J., Miao, C., 2022. Precipitation and nitrogen deposition alter biocrust-vascular plant coexistence in a desert ecosystem: threshold and mechanisms. *Journal of Ecology* 110, 772–783. <https://doi.org/10.1111/1365-2745.13834>.
- Shen, J.X., 2020. Phospholipid biomarkers in mars-analogous soils of the Atacama Desert. *International Journal of Astrobiology* 19, 505–514. <https://doi.org/10.1017/S1473550420000294>.
- Shen, J.X., Smith, A.C., Claire, M.W., Zerkle, A.L., 2020. Unraveling biogeochemical phosphorus dynamics in hyperarid Mars-analogue soils using stable oxygen isotopes in phosphate. *Geobiology* 18, 760–779. <https://doi.org/10.1111/gbi.12408>.
- Sotomayor, D.A., Drezner, T.D., 2019. Dominant plants alter the microclimate along a fog gradient in the Atacama Desert. *Plant Ecology* 220, 417–432. <https://doi.org/10.1007/s11258-019-00924-1>.



- Sutter, B., Dalton, J.B., Ewing, S.A., Amundson, R., McKay, C.P., 2007. Terrestrial analogs for interpretation of infrared spectra from the Martian surface and subsurface: sulfate, nitrate, carbonate, and phyllosilicate-bearing Atacama Desert soils. *Journal of Geophysical Research Biogeosciences* 112, G04S10. <https://doi.org/10.1029/2006JG000313>.
- Swain, T., Hillis, W.E., 1959. The phenolic constituents of *Prunus domestica*. I. The quantitative analysis of phenolic constituents. *Journal of the Science of Food and Agriculture* 10, 63–68. <https://doi.org/10.1002/jsfa.2740100110>.
- Trivedi, P., Leach, J.E., Tringe, S.G., Sa, T., Singh, B.K., 2020. Plant-microbiome interactions: from community assembly to plant health. *Nature Reviews Microbiology* 18, 607–621. <https://doi.org/10.1038/s41579-020-0412-1>.
- UNEP, 1997. *World Atlas of Desertification*, second ed. United Nations Environmental Programme, Nairobi, Kenya.
- Uritskiy, G., Getsin, S., Munn, A., Gomez-Silva, B., Davila, A., Glass, B., Taylor, J., DiRuggiero, J., 2019. Halophilic microbial community compositional shift after a rare rainfall in the Atacama Desert. *ISME Journal* 13, 2737–2749. <https://doi.org/10.1038/s41396-019-0468-y>.
- Voigt, C., Klipsch, S., Herwartz, D., Chong, G., Staubwasser, M., 2020. The spatial distribution of soluble salts in the surface soil of the Atacama Desert and their relationship to hyperaridity. *Global and Planetary Change* 184, 103077. <https://doi.org/10.1016/j.gloplacha.2019.103077>.
- Wang, F., Michalski, G., Luo, H., Caffee, M., 2017. Role of biological soil crusts in affecting soil evolution and salt geochemistry in hyper-arid Atacama Desert, Chile. *Geoderma* 307, 54–64. <https://doi.org/10.1016/j.geoderma.2017.07.035>.
- Waring, S.A., Bremner, J.M., 1964. Ammonium production in soil under waterlogged conditions as an index of N availability. *Nature* 201, 951–952.
- Warren, R.S., Brockelman, P.M., 1989. Photosynthesis, respiration, and salt gland activity of *Distichlis spicata* in relation to soil salinity. *Botanical Gazette* 150, 346–350. <https://doi.org/10.1086/337780>.
- Warren-Rhodes, K.A., Rhodes, K.L., Pointing, S.B., Ewing, S.A., Lacap, D.C., Gómez-Silva, B., Amundson, R., Friedmann, E.I., McKay, C.P., 2006. Hypolithic cyanobacteria, dry limit of photosynthesis, and microbial ecology in the hyperarid Atacama Desert. *Microbial Ecology* 52, 389–398. <https://doi.org/10.1007/s00248-006-9055-7>.
- Warren-Rhodes, K., Ewing, S., McKay, C.P., Rhodes, K.L., 2003. Exploring the Limits to Photosynthetic Life in the Hyperarid Atacama (Chile) and Taklimakan (China) Deserts. American Geophysical Union. Fall Meeting 2003, abstract id. B52B-1042.
- Weiler, M., 2005. An infiltration model based on flow variability in macropores: development, sensitivity analysis and applications. *Journal of Hydrology* 310, 294–315. <https://doi.org/10.1016/j.jhydrol.2005.01.010>.
- Wilhelm, M.B., Davila, A.F., Eigenbrode, J.L., Parenteau, M.N., Jahnke, L.L., Liu, X.L., Summons, R.E., Wray, J.J., Stamos, B.N., O'Reilly, S.S., 2017. Xeropreservation of functionalized lipid biomarkers in hyperarid soils in the Atacama Desert. *Organic Geochemistry* 103, 97–104. <https://doi.org/10.1016/j.orggeochem.2016.10.015>.
- Willers, C., van Rensburg, P.J.J., Claassens, S., 2015. Phospholipid fatty acid profiling of microbial communities—a review of interpretations and recent applications. *Journal of Applied Microbiology* 119, 1207–1218. <https://doi.org/10.1111/jam.12902>.
- Wu, D., Senbayram, M., Moradi, G., Morchen, R., Knief, C., Klumpp, E., Jones, D.L., Well, R., Chen, R.R., Bol, R., 2021. Microbial potential for denitrification in the hyperarid Atacama Desert soils. *Soil Biology and Biochemistry* 157, 108248. <https://doi.org/10.1016/j.soilbio.2021.108248>.
- Yun, K.B.M., Koster, S., Rutter, A., Zeeb, B.A., 2019. Haloconduction as a remediation strategy: capture and quantification of salts excreted by recretahalophytes. *Science of the Total Environment* 685, 827–835. <https://doi.org/10.1016/j.scitotenv.2019.06.271>.
- Zhang, Y., Cai, P., Cheng, G., Zhang, Y., 2022. A brief review of phenolic compounds identified from plants: their extraction, analysis, and biological activity. *Natural Product Communications* 17, 1–14. <https://doi.org/10.1177/1934578X211069721>.
- Ziolkowski, L.A., Wierzchos, J., Davila, A.F., Slater, G.F., 2013. Radiocarbon evidence of active endolithic microbial communities in the hyperarid core of the Atacama Desert. *Astrobiology* 13, 607–616. <https://doi.org/10.1089/ast.2012.0854>.